Available online at www.sciencedirect.com
ScienceDirect
Developmental Biology 309 (2007) 1 – 17
DEVELOPMENTAL BIOLOGY
www.elsevier.com/developmentalbiology

Ol-insm1b, a SNAG family transcription factor involved in cell cycle arrest during medaka development

Eva Candal *, Alessandro Alunni, Violette Thermes, Françoise Jamen, Jean-Stéphane Joly, Franck Bourrat

INRA MSNC Group, DEPSN, Institut Fessard, CNRS, 1 Avenue de la Terrasse, 91198 GIF-SUR-YVETTE, France

Received for publication 21 January 2007; revised 14 April 2007; accepted 26 April 2007
Available online 3 May 2007

Abstract

Through whole-mount *in situ* hybridisation screen on medaka (*Oryzias latipes*) brain, *Ol-insm1b*, a member of the *Insm1/Mlt1 s*ubfamily of SNAG-domain containing genes, has been isolated. It is strongly expressed during neurogenesis and pancreas organogenesis, with a pattern that suggests a role in cell cycle exit. Here, we describe *Ol-insm1b* expression pattern throughout development and in adult brain, and we report on its functional characterisation. Our data point to a previously unravelled role for *Ol-insm1b* as a down-regulator of cell proliferation during development, as it slows down the cycle without triggering apoptosis. Clonal analysis demonstrates that this effect is cell-autonomous, and, through molecular dissection studies, we demonstrate that it is likely to be non-transcriptional, albeit mediated by zinc-finger domains. Additionally, we report that *Ol-insm1b* mRNA, when injected in one cell of two-cell stage embryos, exhibits a surprising behaviour: it does not spread uniformly amongst daughter cells but remains cytoplasmically localised in the progeny of the injected blastomere. Our experiments suggest that *Insm1* is a negative regulator of cell proliferation, possibly through mechanisms that do not involve modulation of transcription.

Keywords: *Insulinoma-Associated-1*; Proliferation; Cell cycle arrest; Mid-blastula transition; Zinc-finger; Transcription factors; Medaka; Fish

Introduction

Cell proliferation and differentiation are essential events in organogenesis. The number of times progenitor cells divide before they exit cell cycle and differentiate largely determines the size of tissues and organs (Caviness et al., 2000; Hardcastle and Papalopulu, 2000; Calle-Mustienes et al., 2002; Kango-Sinh et al., 2002). Defects in cell cycle exit result in lack of cells (if premature) or excess cells, and often underlie tumour progression (Tateno et al., 2001). It is therefore of great fundamental and practical interest to characterise new negative regulators of the cell cycle, which represent potential tumor suppressors. The aim of the present paper is to characterise one such gene.

Our model is the medaka *Oryzias latipes*, a teleost that shares many of the zebrafish characteristics (Wittbrodt et al., 2002). We have used the medaka optic tectum (OT) as a system to identify new cell cycle regulators (Nguyên et al., 2001a; Candal et al., 2005a; Deyts et al., 2005). The medaka OT is a brain cortical structure that grows continuously by addition of columns of cells produced in a proliferative zone restricted to a crescent at its medial, caudal and lateral margin (Nguyên et al., 1999).

Through whole-mount *in situ* hybridisation (WMISH) screens (Nguyên et al., 2001a,b; Deyts et al., 2005), we unravelled a wealth of molecules related to cell proliferation (expression in the marginal proliferative zone; mpz), cell differentiation (expression in the central differentiated zone) and cell cycle arrest (expression in a zone at the border between the two formers). We have thus previously characterised two genes known to be involved in cell cycle arrest, which were strongly expressed in the arrest zone. (1) *Ol-KIP* (*O. latipes*-Kinase Inhibitor Protein; Nguyên et al., 2001b), an orthologue of the cyclin-dependent kinase inhibitor $p57^{KIP2}$ (Dyer and Cepko, 2000; Carey et al., 2002). (2) *Ol-Gadd45γ*, the *O. latipes* orthologue of the mammalian Gadd45γ (a member of the Gadd45 family of growth-arrest and DNA-damage inducible

* Corresponding author. Department of Cell Biology and Ecology, Faculty of Biology, University of Santiago de Compostela, 15782-Santiago de Compostela, Spain. Fax: +34 981 596 904.
E-mail address: ecandal@usc.es (E. Candal).

0012-1606/$ - see front matter © 2007 Elsevier Inc. All rights reserved.
doi:10.1016/j.ydbio.2007.04.038

genes; Candal et al., 2004), the overexpression of which arrests cells before both G1/S and G2/M cell cycle checkpoints.

We also found two potential, albeit poorly characterised, negative growth regulators, i.e., genes with a strong expression in the arrest zone of the medaka OT. These two genes (*Ol-insm1a* and *Ol-insm1b: O. latipes-insm1a* and *1b*) encode 440 and 498 amino acid proteins, respectively, and represent medaka co-orthologues of the mammalian gene *Insm1* (formerly *Insulinoma-Associated-1; IA-1*; Lan et al., 1994), a member of the SNAG transcriptional repressor family.

This family (Grimes et al., 1996) is subdivided into three subfamilies (present results and Tateno et al., 2001): (a) Snail/Slug/Scratch proteins; (b) Gfi1 and Gfi1-related proteins; and (c) Mlt1 and Insm1 proteins. The first two subfamilies contain well-studied transcriptional repressors implicated in a broad range of developmental processes (morphogenetic cell movements, mesoderm and neural crest formation, epithelial–mesenchymal transition, neurogenesis, haematopoiesis…), as well as in tumor progression (Grimes et al., 1996; Sefton et al., 1998; Tong et al., 1998; Stegmann et al., 1999; Nakakura et al., 2001a, b; McGee et al., 2003; Hock et al., 2004; Takahashi et al., 2004; Ashraf et al., 2004; Park et al., 2005; Wu et al., 2005; Fiolka et al., 2006).

The third group consists of two intronless genes, *Mlt1* and *Insm1*, about which much less is known. *Mlt1* is expressed in several normal tissues and is silenced by methylation in liver tumors of MT-D2 mice, suggesting that it functions as a growth or tumor suppressor in liver cells, and possibly also in certain neurones (Tateno et al., 2001). *Insm1* was isolated from a human insulinoma subtraction library (Goto et al., 1992). It is strongly expressed in the developing pancreas, during early Central Nervous System (CNS) development, and in tumours of neuroendocrine origin (Goto et al., 1992; Lan et al., 1993; Breslin et al., 2003; Lukowski et al., 2006) but not in most non-neuroendocrine tumors, nor in normal adult tissues (Lan et al., 1994; Li et al., 1997). *Insm1* is a target gene for *NeuroD1* regulation (and vice versa), suggesting that *Insm1* may play a role during neurogenesis and pancreas organogenesis (Breslin et al., 2002, 2003). It has also been recently reported to be a target of *Neurogenin3* and to be required for normal differentiation of pancreatic endocrine cells *in vitro* (Mellitzer et al., 2006). The role(s) of mammalian Insm1 proteins *in vivo*, and especially in normal CNS development, remains to be clarified.

To further characterise *Ol-insm1* genes, we performed detailed expression and gain-of-function studies. We also performed a clonal ectopic expression analysis and tested the effects of deleted forms of *Ol-insm1b*. Our results clearly point to a previously unravelled role of this gene as a cell cycle arrest factor and shed some light on the molecular mechanism by which this gene is regulating cell cycle withdrawal.

Materials and methods

Fish strains

Medaka embryos and adults of a Carbio strain (kindly provided by Jochen Wittbrodt, EMBL, Heidelberg, Germany) were used in all experiments. Embryos were collected and incubated in Yamamoto's embryo rearing medium (Yamamoto, 1975) at 26 °C and staged according to Iwamatsu (1994).

Ol-insm1a and Ol-insm1b cloning

Ol-insm1a and *Ol-insm1b* were isolated from a cDNA library of medaka embryonic brain (Nguyên et al., 2001b). cDNA was used as template for PCR amplification of the *Ol-insm1a* and *Ol-insm1b* coding regions, using the following primers: pRN3L-insm1a: CGGAATTCCAGCTGTCAGACCACCGCGAACATG; pRN3R-insm1a: ATAGTTTAGCGGCCGCGCTGGTCACGAATCATGTGTGAACAGTCCCGG; pRN3L-insm1b: 5′CGGAATTCCCATCTCCCCAAAGTGCCTTTCTGC3′; pRN3R-insm1b: 5′ATAGTTTAGCGGCCGCCCTCCATTAAAGGCACGAGTTCTGTGTT3′.

DNA fragments of ~1400 bp for *Ol-insm1a* and ~1600 bp for *Ol-insm1b* were purified with QiaexII (Qiagen, Germany), subcloned into pCRII-TOPO (Invitrogen, CA, USA) and sequenced. These fragments were then excised by digestion with *Eco*RI and *Not*I and subcloned into pBluescript-RN3 (Lemaire et al., 1995) to obtain pRN3-*insm1a* and pRN3-*insm1b*.

Sequence analysis

Phylogenetic analyses including the calculation of bootstrap values were done using CLUSTAL W 1.83 at http://www.genebee.msu.su/clustal (Thompson et al., 1994), PHYLIP (Retief, 2000) and GeneBee Phylogenetic Tree Prediction at http://www.genebee.msu.su/services/phtree_reduced.html. Cluster algorithms were used to construct the phylogenetic tree. In the bootstrap the multiple alignment was resampled 100 times.

Whole-mount in situ hybridisation (WMISH)

Sense and antisense digoxigenin-UTP probes were prepared according to Joly et al. (1997). WMISH procedure was performed as described in Deyts et al. (2005). Control sense probes did not lead to any detectable signal. Whole embryos were mounted in 1% methylcellulose (Sigma). For histological analysis, stained embryos were embedded in wax, sectioned at 8 μm on a rotary microtome and counterstained with Nuclear Fast Red.

I-SceI meganuclease-mediated transgenesis

The α1T1pEGFP fusion vector (Hieber et al., 1998) was used to map the functional domains of Ol-Insm1b. Various constructs flanked by I-*Sce*I recognition sites were injected together with the I-*Sce*I meganuclease into one-cell stage medaka embryos as described in Thermes et al. (2002). The following DNA constructs were made: α1T1p-*insm1b* (full sequence) and α1T1p-*VENUS-insm1b* (adding the full sequence coding the fluorescent protein VENUS; Nagai et al., 2002). α1T1p-*insm1b* construct was made by restriction endonuclease digestion of pRN3-*insm1b* and subcloned in frame with the α1T1p-coding sequence. The *VENUS* insert was generated by PCR amplification from pCS2-*VENUS* and subcloned in fusion with *Ol-insm1b*. Clones were verified by sequencing.

Fertilised eggs were injected with 10 ng/μl and 15 ng/μl of α1T1p-*VENUS-Ol-insm1*. For injection, embryos were placed in rows of square-shaped channels made with plastic casts in 1% agarose and kept inside after injection to preserve them ordered. At stage 17 (25 h post-fertilisation; hpf) they were scored and noted for fluorescence. At stage 29 (72 hpf) they were independently (blindly) scored and noted for phenotype.

mRNA microinjections

pRN3-*insm1a* and pRN3-*insm1b* were linearised with *Not*I and transcribed *in vitro* with T3 RNA polymerase using the mMESSAGE mMACHINE kit (Ambion, Applied Biosystems, CA, USA). Following DNAse treatment, RNA was purified with the RNeasy Kit (Qiagen, Germany).

Variable amounts of *Ol-ism1a* and *Ol-insm1b* mRNA, from 450 to 650 ng/μl, were injected into one blastomere at the one-cell stage. Doses lower than 200 ng/μl had no detectable effect on embryonic development. Doses up to 1300 ng/μl had no lethal effects. After injection, embryos were returned at

26 °C. We used basal salt solution (BSS) and *EGFP* mRNA (500 ng/μl) as control solutions.

Clonal analyses were performed by injecting of *Ol-insm1b* mRNA (500 ng/μl) in a central blastomere at the 32-cell stage. Control embryos were injected with 0.8 μg/μl of MO-insm1b-C_F alone.

DAPI staining

Pre- and post-mid-blastula transition (MBT) embryos were fixed for 2 h in 4% paraformaldehyde (PFA) and dechorionated, and blastoderm was separated from the yolk. Before MBT, cells were counted with the Metamorph® Imaging System software, following incubation with DAPI (Sigma; 300 nM in PBS for 30 min). After MBT, DAPI-stained cells were microscopically analysed for evidence of apoptosis.

TUNEL assay

VENUS-Ol-insm1b mRNA (500 ng/μl; see below for mRNA transcription and recovery) was injected in one blastomere at the two-cell stage. Development of injected embryos was arrested at 9 hpf (stage 11; MBT) by fixation with 4% PFA and glutaraldehyde 0.05% for 48 h at 4 °C. Embryos were mechanically dechorionated in PBS and *in toto* analysed for apoptosis. Fixed-embryos were permeabilised with 0.1% sodium citrate, labelled for DNA strand breaks using the *In Situ* Cell Death Detection kit (TUNEL, Roche Molecular Biochemicals). Staining substrate was Fast Red (Roche Molecular Biochemicals). Whole embryos were observed under a Leica MZFL III dissecting microscope.

Morpholinos experiments

A fluorescein-conjugated antisense morpholino oligonucleotide (MO-insm1b-F: 5′TTTTTACCAGGAATCCTTTGGGCAT3′) was designed to target the sequence containing the initiation codon of *Ol-insm1b* (Gene Tools, USA). Various amounts of MO (from 4 to 16 μg/μl) were injected into one blastomere of one-cell stage embryos. A mispaired morpholino (MO-insm1b-C_F: 3′TTTTTAGCACCGAATGCTTTCGGGAT5′; mispaired bases are underlined) was used as control.

Flow cytometry

Ol-insm1b mRNA-injected and uninjected embryos were frozen in liquid nitrogen at MBT (stage 10) and dechorionated in Galbraith buffer (Galbraith et al., 1983). Nuclei were separated from debris by filtration through a 50-μm nylon mesh. Filtrates were treated with RNase A (100 μg/ml) and stained with 10 μg/ml DAPI (Sigma). Nuclei (3.000) were analysed with an EPICS Elite ESP flow cytometer. Nuclei from adult medaka liver cells (G1 arrested) were used for calibration of the 2N DNA population. DNA content histograms were resolved by the MultiCycle AV software. Histograms were obtained using MultiCycle AV software.

Functional domains deletions and fusion proteins

Deletions of *Ol-insm1b* were prepared: (1) pRN3-*insm1b*ΔSNAG (lacking three of the seven amino acids of the SNAG domain) was obtained by enzyme restriction of pRN3-*insm1b* with *Xcm*I and *Sma*I. (2) pRN3-*insm1b*ΔNH_2 (deletion of 207 amino acids of the amino-terminal half containing the SNAG domain) was generated by PCR amplification from pCRII-TOPO-Ol-insm1b using the following primers: pRN3L_a-*insm1b*ΔNH2: 5′GAATTCGCCACCATGCTCGGGCTCAAAATCAAAGAGGGG3′ and pRN3R_a-insm1b: 5′ATAGTTTAGCGGCCGCCCTCCATTAAAGGCACGAGTTCTGTGTT3′; the fragment was excised with *Eco*RI and *Not*I and cloned into pBluescript-RN3. (3) pRN3-*insm1b*Δzf1–2 (which lacks the first two zinc-finger domains) was obtained by enzyme restriction of pRN3-*insm1b* with *Bsi*WI and *Nde*I. (4) pRN3-*insm1b*Δzf1–5 (lacking the carboxyl-terminal half containing the five zinc-finger domains) was generated by enzyme restriction of pRN3-*insm1b* with *Bsi*WI and *Not*I. Plasmids linearisation, *in vitro* transcription, mRNA recovery and mRNA microinjections were performed as described above.

Fusion proteins were obtained from the following constructs: (1) pRN3-*VENUS-Ol-insm1b*; the *VENUS-Ol-insm1b* fragment was excised from α1T1p-*VENUS-insm1b* with *Bam*HI and *Not*I and cloned into pBluescript-RN3. (2) pRN3-*VENUS-Ol-insm1b*ΔNH_2; VENUS was excised from pRN3-*VENUS-Ol-insm1b* with *Bst*Y and *Age*I and subcloned in frame into pRN3-*insm1b*ΔNH_2. (3) pRN3-*VENUS-Ol-insm1b*Δzf1–2 was obtained by enzyme restriction of pRN3-*VENUS-Ol-insm1b* with *BsiW*I and *Nde*I. Plasmids were linearised with *Kpn*I, *in vitro* transcribed with the mMESSAGE mMACHINE T3 kit (Ambion, Applied Biosystems, CA, USA), the RNA was lithium chloride precipitated following manufacturer's instructions, and mRNA microinjections were performed as described above.

Results

Cloning and sequence analysis

In the course of a WMISH screen on the medaka OT (Nguyên et al., 2001b; Deyts et al., 2005), we isolated two poorly characterised genes that exhibited a strong expression in the OT arrest zone: CDOL_001_1270 and CDOL_000_0598, the predicted products of which were 56.4% identical at the amino acid level. BLAST search analyses showed that CDOL_001_1270 is similar to mouse and human insulinoma-associated 1 (Insm1; formerly IA-1) intronless proteins (48.7% and 52.7% identity). CDOL_000_0598 is also similar to these mammalian proteins (46.4% and 49.4% identity). We thus named these genes *Ol-insm1a* and *Ol-insm1b*, respectively. The vertebrate Insm1 family also contains two zebrafish members (Dr-Insm1a and Dr-Insm1b) that are 63.3% and 60.9% identical to Ol-Insm1a and Ol-Insm1b. Insm1 belongs to a highly conserved subgroup of zinc-finger proteins, the SNAG transcriptional repressor family (Fig. 1A), characterised by a seven amino acid SNAG repressor motif in the NH2 terminal and four-to-six C2H2-type zinc-finger motifs in the COOH-terminal half (Fig. 1B).

The SNAG family consists of 20 proteins (Tateno et al., 2001). A survey of available protein databases unravelled two additional members (Scratch 1 and Scratch 2). Two other members were recently described in zebrafish (Dr-Insm1a and Dr-Inms1b; Lukowski et al., 2006). Fig. 1A shows the phylogenetic relationship amongst SNAG proteins (the analysis of their full sequences was made as described in Materials and methods). The resulting tree indicates that the SNAG family is made of three subfamilies: (a) Snail/Slug and Scratch proteins, (b) Gfi1 proteins and (c) Insm1/Mlt1 proteins. Fig. 1B shows the multiple alignments of Ol-Insm1b and Ol-Insm1a with other reported members of the Insm1/Mlt1 subfamily.

Ol-insm1b expression pattern in embryos and adult CNS

This study is focussed on *Ol-insm1b*: indeed, in our functional analysis *Ol-insm1a* appeared to behave in a similar albeit weaker way than *Ol-insm1b* (see below).

Ol-insm1b transcripts are not detected during early cleavages and gastrula stages, when all cells proliferate actively, neither by WMISH nor by real-time PCR analysis (data not shown). *Ol-insm1b* is first detected in the rostral pole at early neurula stage (stage 18; optic bud formation) (Fig. 2A). *Ol-insm1b* expression then increases throughout the brain, especially in the telen-

cephalon and the rhombic lips (stage 24; 16 somites; Fig. 2B). At stages 28 and 30 (30 and 35 somites; Figs. 2C, D and G–I), *Ol-insm1b* is highly expressed in the telencephalon (Fig. 2G), in the OT and midbrain tegmentum (Figs. 2H, I) and in the hindbrain, where it is expressed in a characteristic banded pattern (Figs. 2C, D, H). At these stages, *Ol-insm1b* is strongly

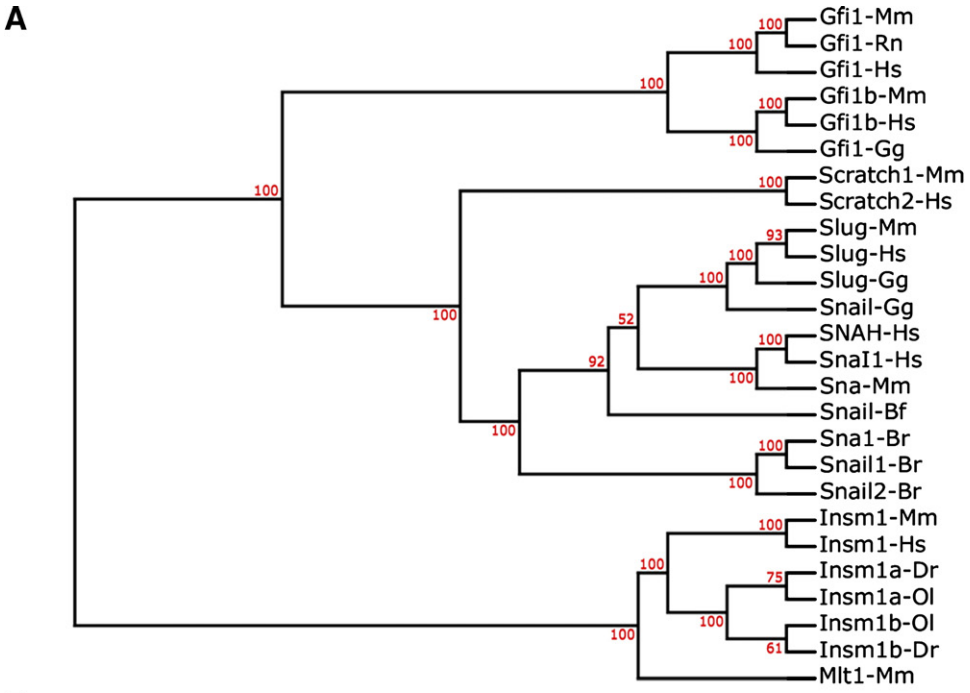

B

```
                SNAG
  Mlt1_Mm   MPRGFLVKHTKRSGS-SYRARPVEP------------------------LFPPPGPLAAQSSPEEPGRGLLGSPCLAPPQD---DAEWG
 Insm1_Hs   MPRGFLVKRSKKSTPVSYRVRGGEDGDRALLLSPSCGGARAEPPAPSPVPGPLPPPPPAERAHAALAAALACAPGPQPPPQGPRAAHFG
Insm1a_Dr   MPRGFLVKRNKKATPVSYRVRSEEDE-----------------------------------QGAFVAQDVPCARRPVS----PVQFG
Insm1b_Dr   MPKGFLVKRNKKAALISYRIRTDEDG-----------GPTPECPIA---QIALSSPAPSASKPDSILLAFPSAGAEAPVP-VHKPVQFG
Insm1b_Ol   MPKGFLVKRNKKCAHVSYRTRSEEDD-----------LQEPPTPAALPRQTDHSPPMSVASSPGRASASPDFTAAEAPVARLEKPTQFG
Insm1a_Ol   MPRGFLVKRNKKTIPVSYRVRSDDEE-----------PDQASVDAPPLLPPSSSSSAHFASIPVRTPTPSFGAAATAPDQDA-KPIQFG

  Mlt1_Mm   AGGGDGPG--PSPAKPAGPELRR--AFEERC-CRSPVSAESFPSATAF---------------------CSAAPAAVTSGEELQPPDV-
 Insm1_Hs   NPEAAHPAPLYSPTRPVSREHEKHKYFERSFNLGSPVSAESFPTPAALLGGGGGGGASGAGGGGTCGGDPLLFAPAELKMGTAFSAGAEA
Insm1a_Dr   NPETVYRA-MYSPTRPVSREHER-ACLERRFNLGSPISAESFPAAP-----------------NCSDQ----APVDLKIGTSNSNRTG-
Insm1b_Dr   NPEAVYQA-LYSPTRPVSKDHDR-KYFERSLNLGSPISAESFPTPASL---------------TSLDHHLLFAPVDLKIGTSNSNRSG-
Insm1b_Ol   NPETECQA-LYSPTRPISKEHDK-GYFEQSFSLGSPISAESFPTPASL---------------SGLDH-ILYAPVDLKIGTSNSSRSGI
Insm1a_Ol   NPETVYRG-LYSPTRPVSQDHDR--YLERRFNLGSPVSAESFPTPAAL---------------TALGH--LFAPVDLKIGSRTSNHAE-

                                                NLS
  Mlt1_Mm   -------PVSVPIPVPGPAPKGLDRRGKGAPICAS-APAAVRKPKAVRRLSFAQEVIISPVLGLKIKEEEPGA-PARALGGVRTPLGEFI
 Insm1_Hs   ARGPGPGPPLPPAAALRPPGKRPPPPTAAEPPAKAVKAPGAKKPKAIRKLHFEDEVTTSPVLGLKIKEGPVEA-PRGRAGGAARPLGEFI
Insm1a_Dr   -------------------TTVTTKRPASDTERK--GKPASKKAKAMRKLQFEDEMTTSPVLGLKIKEGPVEQKPRSQCASGDKPPGEFV
Insm1b_Dr   ----------TASGAHAPAIRTGAKRPSADAAERKVSSKSAKKPKAIRKLNFEDEVTTSPVLGLKIKEGPVDLKPRPSSGGTNKPLGEFI
Insm1b_Ol   TSTTTSSTTTSSSSLPGPSNRVATKRSAGDAAERK-SKSSSKKPKAIRKLNFEDEMTTSPVLGLKIKEGPVEVKPRAQSSGGNKPLGEFV
Insm1a_Ol   ----------ASASFSGKIPISGAKRPPSDP-ERK-GKPPSKKTKAIRKLHFEDDVTTSPVLGLKIKEAPVDQKQQPNTSDQH-PLGEFV

                zf1                     zf2
  Mlt1_Mm   CQLCKHQYADFFALAQHRCSRIVRVEYRCPECDKVFSCPANLASHRRWHKPRPTPACAASKPPHAPLTPPDPSLATGKENGRVPRTDDQH
 Insm1_Hs   CQLCKEEYADPFALAQHKCSRIVRVEYRCPECAKVFSCPANLASHRRWHKPR--------PAPAAARAPEPEAAARAEAEPAGGGSDRD
Insm1a_Dr   CQLCREAYADPFSLAQHKCSRIVRIEYRCPECDKLFSCPANLASHRRWHKPK--------QSAESNKTPAPEKEETS---------SDRD
Insm1b_Dr   CQLCKEEYSDPFSLAQHKCSRIVRVEYRCPECEKVFSCPANLASHRRWHKPR-------VQSAPKQALQPAKPFPEELR---AEFPSDRD
Insm1b_Ol   CQLCEEAYADPFSLAQHKCSRIVRVEYRCPECDKMFSCPANLASHRRWHKPRTTNGAPAMPAAPGIKPEMAKIMPMGVKSDEAKDMSDRE
Insm1a_Ol   CQLCREAYADPFSLAQHKCSRIVRVEYRCPECDKVFSCPANLASHRRWHKPK--------PQSGGHHLESDKVANKTAP-DDTKDCSDRD

                                                zf3
  Mlt1_Mm   PQAPDSSGDGQHRDSAARPGLQALVYPEAARPQAPYPEVILGRHGPGSSGASAGATSEVFVCPYCHKKFRRQAYLRKHLGTHE-------
 Insm1_Hs   TPSPG-----------------------------------------GVSESGSEDG----LYECHHCAKKFRRQAYLRKHLLAHH-------
Insm1a_Dr   TPSPG-----------------------------------------LSESGSEDG----LYDCQHCGKKFKRQAYLKKHVTAHH-------
Insm1b_Dr   TPSPG-----------------------------------------LSESGSEDG----LYDCQHCGKRFKRQAYLRKHILGHQ-------
Insm1b_Ol   TPSPG-----------------------------------------PSESGSEDG----SYDCQYCGKRFKRQAYLRKHIMGHRVLQKKVL
Insm1a_Ol   TPSPQ-----------------------------------------PSESGSDDG----LCDCNQCGKRFKRQAYLRKHLASQH-------

                                                zf4
  Mlt1_Mm   ----------------------------TGSARAPTPGFGSERTAPLTF-A------CPLCGAHFPSADIREKH-RLWHAVREELLLPALV
 Insm1_Hs   -----QALQAKGAPLAPPAEDLLALYPGPDEKAPQEAAGDGEGAGVLGLSASAECHLCPVCGESFASKGAQERHLRLLH------------
Insm1a_Dr   ----------------DAP-------------------EKPQSHAPLNLSAS-ECHLCPVCGENFPSRMSQERHIRLQH------------
Insm1b_Dr   ----------------ALQNQILGEAFRSAESPDAMPSEDRQSPAPLNLSPA-DCLTCPACGEKLPNRASLERHLRPLH------------
Insm1b_Ol   EEHGFQTSDRATEQAPVSSSSSSSLASSSSSSSSSSSSSEVASNQSPLNLSPV-DCLLCPVCGESFTSRAGQERHLRLMH------------
Insm1a_Ol   ----------------GSP--------KPAREDDARPCE--QSAAPLNLSAS-TCHLCPVCGEKFSSRGSQERHIRLLH------------

                zf5
  Mlt1_Mm   GAPSEAGPGGASDGSAQQIFSCKYCPSTFFSSPGLTRHINKCHPSESRQVLLLQMPLRPGC
 Insm1_Hs   --------------A-AQVFPCKYCPATFYSSPGLTRHINKCHPSENRQVILLQVPVRPAC
Insm1a_Dr   --------------S-AQVYPCKYCPAMFYSSPGLTRHINKCHPSENRQVILLQMPVRPAC
Insm1b_Dr   --------------DDAQAFPCKFCPATFYSSPGLTRHINKCHPTENRQVILLQMPVRNAC
Insm1b_Ol   --------------S-SQIYPCKYCPATLYSSPGLTRHINKCHPSENRQVILLQMPVRPAC
Insm1a_Ol   --------------S-SHMYPCKYCPAVFYSSPGLTRHINKCHPSENRQVILLQMPLRPAC
```

Fig. 1. (A) Phylogenetic tree of the SNAG family; SNAG proteins are subdivided in three subfamilies: Gfi1-related, Snail/Slug/Scratch and Mlt1/Insm1 proteins. (B) Multiple alignments of Ol-Insm1a and Ol-Insm1b with members of the Insm1/Mlt1 subfamily. Conserved SNAG, NLS and zinc-finger domains are indicated. Phylogenetic analysis was done using CLUSTAL W 1.83 with a PHYLIP output format. Cluster algorithms were applied to construct the phylogenetic tree at the GeneBee page (see Materials and methods for details). Bootstrap values are expressed in percentages and placed at nodes.

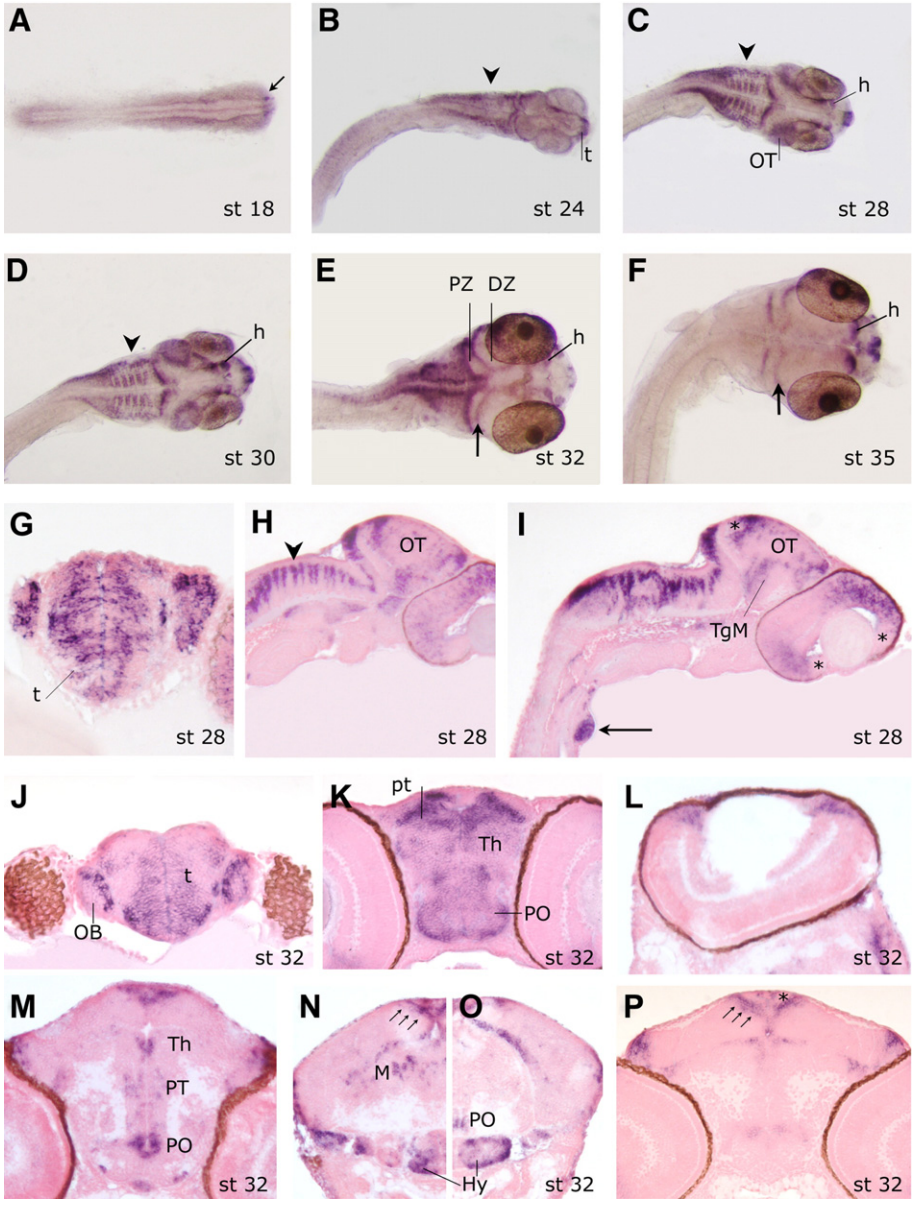

Fig. 2. Expression pattern of *Ol-insm1b* after ISH in whole-mount embryos (A–F), and in sagittal (H, I) and transverse (G, J–P) sections of medaka embryos at the indicated stages. Arrow in (A) indicates *Ol-insm1b* expression in the rostral pole of the embryo. Arrowheads in (B–D, H) indicate *Ol-insm1b* expression in the rhombic lips. Arrows in (E, F, N, P) indicate the arrest zone of the optic tectum. Arrow in (I) indicates *Ol-insm1b* expression in the pancreas. Stars in (I, P) indicate the proliferative zones of the retina and OT. DZ, differentiation zone; h, habenula; Hy, hypothalamus, M, midbrain; OB, olfactory bulb; OT, optic tectum, PO, preoptic area; pt, pretectum; PT, posterior tubercule; PZ, proliferation zone; t, telencephalon; TgM, tegmentum; Th, thalamus.

expressed in the arrest zone in the medaka OT (Figs. 2C, D, H); it is also present in some scattered cells in the central area of the OT where the first signs of differentiation appear (Fig. 2H). In the retina, *Ol-insm1b* is widely expressed throughout the differentiating zone, absent from the marginal proliferative zone and from the most mature central (already differentiated) zone of the retina (Fig. 2I). Outside the brain, *Ol-insm1b* is strongly expressed in the pancreas (Fig. 2I). Neural *Ol-insm1b* expression decreases as development proceeds and cells differentiate (Fig. 2E). In transverse sections through the brain at stage 32 (34–35 somites; Figs. 2E and J–P), *Ol-insm1b* is detected in the olfactory bulbs and in the telencephalon (especially in its ventral area; Fig. 2J), in pretectal, thalamic and preoptic regions (Figs. 2K, M, O), in the primordial right and left habenula (Figs. 2C–F), in the suprachiasmaticus nucleus, in the posterior tubercle (Fig. 2M), in the rostral and caudal hypothalamus (Figs. 2N, O), in some midbrain–tegmentum nuclei (Fig. 2N), in the torus semicircularis and in a small number of hindbrain nuclei. In the OT (Fig. 2P), *Ol-insm1b* expression is restricted to the limit between the proliferative and post-mitotic zones and absent from proliferating cells in its caudal, ventrolateral and dorsomedial margins. The same pattern is observed in the retina (Fig. 2L), where mRNA is located at the border between the mature central retina and the marginal proliferative zone. *Ol-insm1b*

expression decreases from stage 35 onwards (Fig. 2F), especially in the hindbrain.

Ol-insm1b is also strongly expressed in the adult brain (Figs. 3A, B); it generally remains expressed in the domains where it showed an embryonic expression and is turned on in some additional territories (Figs. 3C–K). Series of horizontal, sagittal and transverse sections allowed us to observe labelled cells in the olfactory bulbs and in both the ventral and dorsal telencephalon (Figs. 3C–E), in the suprachiasmaticus nucleus (Fig. 3E), in preoptic, thalamic and pretectal regions (Figs. 3E–G). *Ol-insm1b* shows a peculiar asymmetric expression in the adult habenula (left side only), whereas it is expressed sym-

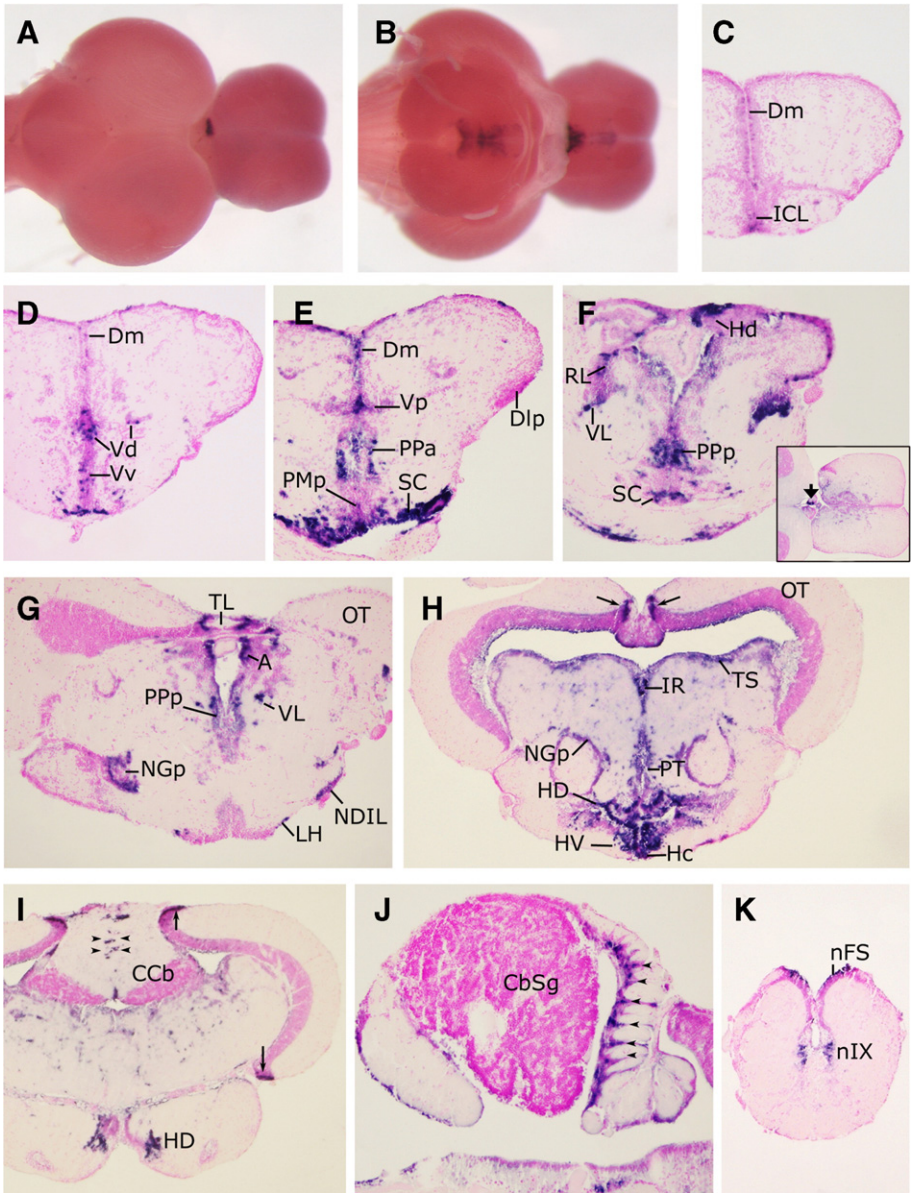

Fig. 3. Expression pattern of *Ol-insm1b* in adult medaka brain after WMISH in dorsal (A) or ventral view (B), and in sagittal (J), transverse (C–I, K) or horizontal (inset in F) sections. Labelled cells are found in the olfactory bulbs and in both the ventral and dorsal telencephalon (C–E), in the suprachiasmaticus nucleus (E), in preoptic, thalamic and pretectal regions (E–G), in the left habenula (where *Ol-insm1b* mRNA is strongly and asymmetrically expressed; F and inset within; compare with Figs. 2C–F showing a symmetrical habenular expression of *Ol-insm1b* during embryonic development), in the anterior and posterior tubercle (H) and in the rostral and caudal hypothalamus (G–I); *Ol-insm1b* mRNA is also detected in some midbrain–tegmentum nuclei (H); in the dorsal midbrain, *Ol-insm1b* mRNA expression is observed in the torus semicircularis and in the limit between the proliferative and post-mitotic zones of the OT (H, I); *Ol-insm1b* mRNA is observed in the cerebellum (I, J) and in a small number of hindbrain nuclei (K). Arrow in (F) indicates the asymmetrical labelling in the left habenula. Arrows in (I) indicate the arrest zone of the optic tectum. A, anterior nucleus of the diencephalon; CbSg, granular stratum of CCb; CCb, cerebellar body; Dlp, area lateroposterior of the diencephalon; Dm, area medial of the dorsal telencephalon; Hc, periventricular caudal hypothalamus; Hd, dorsal habenula; HD, periventricular dorsal hypothalamus; HV, periventricular ventral hypothalamus; ICL, inner cellular layer of the OB; IR, inferior rectus of nucleus of the oculomotor nerve; LH, lateral nucleus of the hypothalamus; NDIL, nucleus diffusus of the hypothalamic anterior lobe; nFS, nucleus of the fasciculus solitarius; NGp, posterior glomerulosus nucleus; nIX, nucleus of the glosso-pharingeal nerve; OT, optic tectum; PMp, preoptic magnocellular posterior nucleus; PPa, preoptic parvocellular anterior nucleus; PPp, preoptic parvocellular posterior nucleus; PT, posterior tubercle; RL, rostrolateral nucleus of the diencephalon; SC, suprachiasmatic nucleus; TL, torus longitudinalis; TS, torus semicircularis; Vd, dorsal area of the ventral telencephalon; VL, ventrolateral nucleus of the diencephalon; Vp, posterior area of the ventral telencephalon; Vv, ventral area of the ventral telencephalon.

metrically in the development of this structure (compare Figs. 2C–F with Figs. 3A, F and inset within). *Ol-insm1b* mRNA is also expressed in the anterior and posterior tubercle (Fig. 3H) and in the rostral and caudal hypothalamus (Figs. 3H, I); *Ol-insm1b* mRNA is also detected in some midbrain–tegmentum nuclei (Figs. 3H, I); in the dorsal midbrain, *Ol-insm1b* mRNA expression is observed in the torus semicircularis and in the limit between the proliferative and post-mitotic zones of the OT (Fig. 3H); *Ol-insm1b* mRNA is observed in the cerebellum (Figs. 3I, J) and in a small number of hindbrain nuclei (Fig. 3K).

By analogy with genes previously characterised (Nguyên et al., 2001a,b; Candal et al., 2004, 2005a), the continued expression of *Ol-insm1b* at the border between the mature central zone and the marginal proliferative zone of both the OT and the retina strongly suggested that *Ol-insm1b* was potentially involved in negative growth control in the nervous system. We began the analysis of its function by attempting to inhibit its expression with morpholinos. We got no detectable effects whatsoever on cell cycle rate and number of cells after one-cell stage injection of the vehicle solution only, after injection of the specific morpholino MO-insm1b-$_F$ at 8 μg/μl or after injection of the mismatch morpholino MO-insm1b-C_F at the same concentration (data not shown).

We thus turned to ectopic expression experiments and began by attempting to express *Ol-insm1b* in proliferating cells of the nervous system.

Ol-insm1b affects late embryonic neural development

To ectopically express *Ol-insm1b* in the developing medaka nervous system, we used I-*Sce*I meganuclease-mediated transgenesis, the high efficiency of which allows analysing the effects of overexpression of a particular gene in mosaic (F0) injected embryos, without establishing stable transgenic fish lines. This method has proven to be quick, powerful and amenable to quantification in fish and amphibian models (Thermes et al., 2002; Grabher et al., 2004; Pan et al., 2006; Ogino et al., 2006). We injected fertilised eggs with 10 ng/μl of a DNA construct (α1T1p-*VENUS*-*Ol-insm1b*) where the expression of a VENUS-Ol-Insm1b transgene is driven by the α1-tubulin promoter, which directs expression specifically in the proliferating neural progenitors (Gloster et al., 1994, 1999). A mosaic expression of VENUS-Ol-insm1b was first observed at the beginning of neurulation (25 h post-fertilisation (hpf), stage 17), when the promoter becomes active. Embryos were grouped in three classes according to the amount of fluorescent, transgene-expressing cells in the central nervous system. Embryos showing no VENUS-Ol-Insm1b-expressing cells were classified as negative ("absent"); embryos in which only a small amount of cells expressed VENUS-Ol-Insm1b were classified as "weak"; embryos with an almost ubiquitous VENUS-Ol-Insm1b expression in the nervous system were classified as "strong". They were allowed to develop up to stage 29 (72 hpf) and their phenotypes recorded (see Table 1). Embryos were judged to be "small" or to "have brain malformations" when they were reduced in size or showed altered and/or delayed development with respect to normal embryos (Candal et al., 2005c; Candal, 2002). Most embryos showing no fluorescence at the beginning of neurulation developed normally (95.2%; Table 1 and Figs. 4A, B), and only a small percentage was reduced in size (4.8%), without severe brain malformations. None of the embryos showing a weak transgene expression developed normally, 44.4% were reduced in size and 55.6% showed additional brain abnormalities (Table 1). Among the embryos exhibiting a strong transgene expression, 16.7% showed a reduction in size and no brain abnormalities, whilst 83.3% exhibited size reduction and severe brain anomalies (Table 1 and Figs. 4C, D). This effect was dose-dependent since the percentage of embryos showing both reduction in size and critical brain malformations increased when 15 ng/μl of α1T1p-*VENUS*-*Ol-insm1b* was injected at the one-cell stage (see Table 1).

Since the main result of these experiments is an overall reduction in CNS size following *Ol-insm1b* over-expression in neural progenitors, it further points to a role of this gene in negative cell cycle control in brain development. To analyse this effect in more details, we turned to mRNA injections in early embryos. This method can also be used to evaluate the role of the different domains of a molecule. Given the stability of the mRNAs in such experiments, we expected to observe differences between injected and control embryos at about the stage when *Ol-insm1b* is normally expressed, i.e., at early neurula.

Ectopic expression of Ol-insm1b causes cell cycle arrest in early embryos

Ol-insm1b mRNA (500 ng/μl) was injected at the one-cell stage and a developmental delay was observed (Table 2 and Fig. 5). At 2.5 hpf (stage 5; 8-cell stage), 71.4% of mRNA-injected embryos were delayed ($n=207$). To quantify the degree of delay in cell divisions, embryos were allowed to develop at 26 °C after injection, and cell numbers were counted from stage 4 (2 hpf; four-cell stage) until stage 9 (6 hpf; about 512 blastomeres in control embryos).

The number of cells in delayed embryos was significantly reduced when compared to control embryos, which divided normally (Table 2 and Figs. 5A, B). Moreover, cells in the

Table 1
Late dose-dependent effects of *Ol-insm1b* on development (transient transgenesis experiments)

			Phenotype (stage 29)		
			wt-like	Small size	Small size and brain malformations
Fluorescence (stage 17)	10 ng/μl $n=36$	Absent	95.2%	4.8%	0
		Weak	0	44.4%	55.6%
		Strong	0	16.7%	83.3%
	15 ng/μl $n=29$	Absent	81.8%	18.2%	0
		Weak	0	63.6%	36.4%
		Strong	0	0	100%

Values indicate the percentage of embryos of each phenotype showing none, weak or strong transgene expression after injection of α1T1p-*VENUS*-*Ol-insm1b*. A statistically significant relation was found between the strength of fluorescence and the severity of altered phenotype after MBT ($P<0.0005$, Chi-square test). *n*: number of injected embryos.

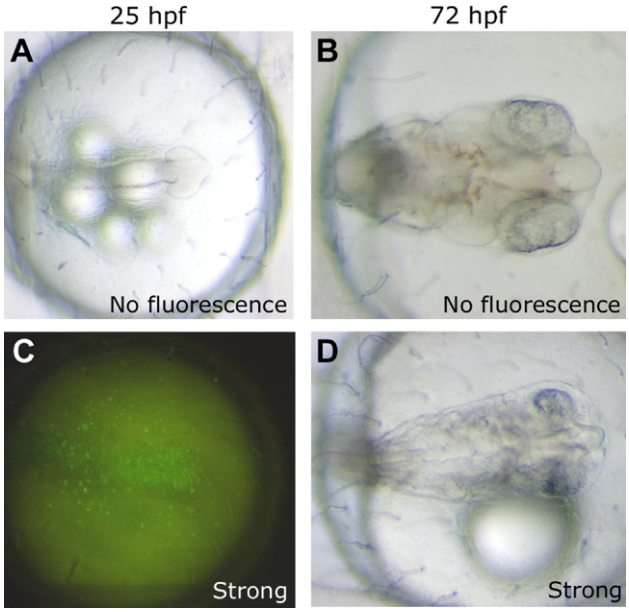

Fig. 4. *Ol-insm1b* affects medaka development. After α1T1p-VENUS-*Ol-insm1b* injection, embryos at stage 17 (25 hpf) were grouped according to transgene expression: absent (A, bright field), weak (not shown) or strong (C). Most of non-fluorescent embryos developed normally until stage 29 (72 hpf, B), whereas all strongly transgene-expressing embryos displayed severe brain anomalies and/or became reduced in size (D).

mRNA-injected embryos were larger. Divergence in the number of cells between *Ol-insm1b* mRNA- and control-injected embryos increased as development proceeded (100% of embryos were delayed at 4 hpf, $n=175$; Table 2). At 6 hpf (stage 9), both *Ol-insm1b* mRNA and BSS injected embryos were fixed, stained with DAPI, and nuclei were counted. *Ol-insm1b* mRNA-injected embryos showed a severe decrease in cell number, as compared with control embryos (276±20.3 versus 539±21.7; Table 2; see also Figs. 5C, D at 9 hpf).

To determine if Ol-Insm1b induced apoptosis, injected embryos were allowed to develop until stage 11 (9 hpf, late blastula) when apoptotic pathways become active (Hensey and Gautier, 1997; Carter and Sible, 2003). They were stained with DAPI that allow identification of chromatin condensation, nuclear shrinkage and formation of apoptotic bodies (Huynh and Teel, 2000; Zong et al., 2003; Candal et al., 2004, 2005b). No signs of apoptosis were ever detected (Figs. 5C, D).

Table 2
Ectopic expression of *Ol-insm1b* during pre-MBT development

	2.5 hpf (st. 5), $n=207$ [a]	4 hpf (st. 8), $n=175$ [b]	6 hpf (st. 9), $n=177$ [c]
BSS	8±0	61.3±3.01	539±21.7
Ol-insm1b mRNA (500 ng/μl)	5.7±1.25	35.2±7.82	276±20.3

Values indicate the mean number of cells (with standard deviations) as computed in *Ol-insm1b* mRNA-injected and control (BSS-injected) embryos at different developmental stages. Differences amongst *Ol-insm1b* mRNA-injected and control embryos were significant ($P<0.0001$, Student's t test) for each point of observation (in hours post-fertilisation; hpf). *n*: total number of injected embryos.

[a] 207 from 290 embryos (71.4%) were retarded.
[b] 175 from 175 embryos (100%) were retarded.
[c] 177 from 177 embryos (100%) were retarded.

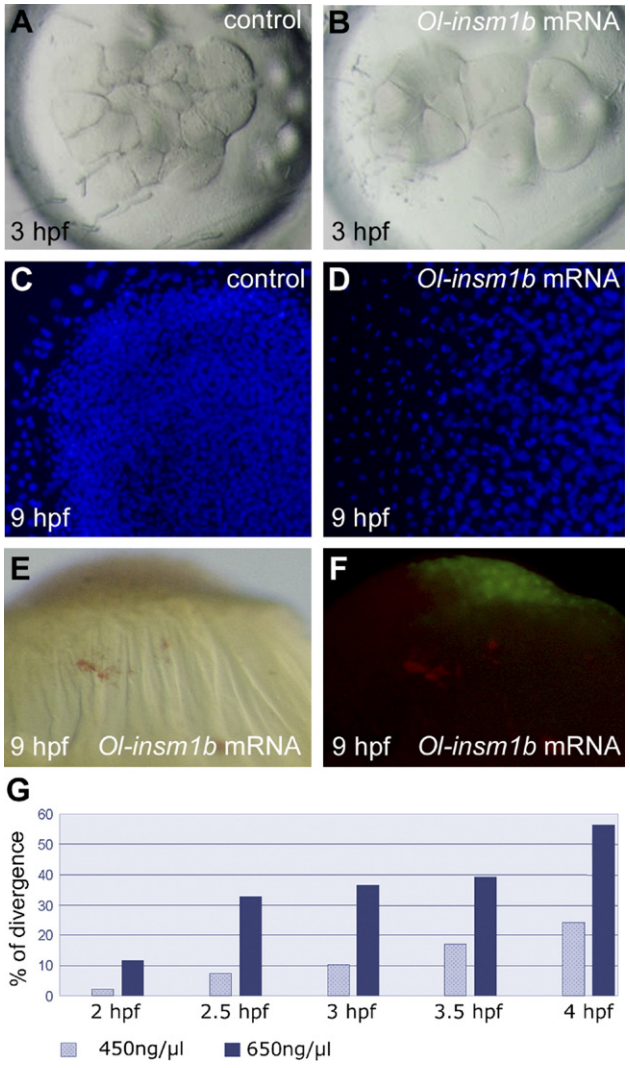

Fig. 5. Ectopic *Ol-insm1b* expression causes cell cycle delay. (A, B) Dorsal views of early embryos (3 hpf). In the *Ol-insm1b* mRNA-injected embryos (B), the number of cells is reduced and cells are larger respective to control embryos (A). (C, D) DAPI staining at the late blastula stage (9 hpf). The number of cells is reduced in the *Ol-insm1b* mRNA-injected embryos, without evidence of cell death. (E, F) TUNEL staining at the late blastula stage (9 hpf). Fast Red-stained (apoptotic) cells were only observed in extra-embryonic tissues (E); VENUS-Ol-Insm1b expressing cells (in green) are devoid of Fast Red staining (F). (G) Percentage of divergence in numbers of cells obtained after injection of different concentrations of *Ol-insm1b* mRNA: the effect of *Ol-insm1b* is dose-dependent.

Injected embryos were additionally injected with *VENUS-Ol-insm1b* mRNA (a construct that allows direct observation of the mRNA transcripts; see results below) and analysed for apoptosis by the TUNEL method as described in Materials and methods. No apoptosis above basal levels was detected at 9 hpf neither in wild-type-like embryos (data not shown) nor in *Ol-insm1b* mRNA-injected embryos, although the level of apoptosis was slightly increased in extra-embryonic tissues (Figs. 5E, F).

We then tested the effect of increasing amounts of *Ol-insm1b* mRNA at different embryonic stages (Fig. 5G). The percentage

of divergence was calculated as $[(nC-nRi)/nC]\times 100$, where nC is the mean number of cells in control embryos and nRi is the mean number of cells in *Ol-insm1b* mRNA-injected embryos. Divergence in the number of cells between *Ol-insm1b* mRNA- and control-injected embryos increased as development proceeded and this effect was clearly dose-dependent.

We examined the effects of these *Ol-insm1b* injections on late development. Injected embryos progressed through gastrulation but their development was severely affected: when compared with control embryos (Figs. 6A, B) they exhibited a delayed epiboly at 18 hpf (stage 15, Fig. 6C) and a reduced size at 42 hpf (stage 23, Fig. 6D), probably as a consequence of the early decrease in cell number.

A similar analysis was performed by injecting *Ol-insm1a* mRNA (500 ng/µl). Early cleavages were also affected, but to a lesser extent, as shown by the reduction in cell numbers: 346±57 for *Ol-insm1a* mRNA *versus* 276±29 for *Ol-insm1b* mRNA injection, at the same dose and the same developmental stage (6 hpf; stage 9; data not shown). Since *Ol-insm1a* appeared to have similar (but weaker) effects on cell division, all assays were carried out with *Ol-insm1b*.

Specificity of Ol-insm1b mRNA effect

We wondered whether this strong anti-proliferative effect was specific to *Ol-insm1b* (and *Ol-insm1a*) or was shared by other genes of the SNAG family, the functions of which are rather poorly documented. We thus cloned *Ol-Mlt1*, the medaka homologue of the mouse *Mlt1*, which represents the "closest relative" to the *Ol-insm1* genes in the SNAG family (see Fig. 1). *Ol-Mlt1* mRNA was injected at the one-cell stage in the same conditions as described above for *Ol-insm1b*. Embryos were monitored from 2 hpf to 6 hpf, and from the beginning of neurulation onwards. No significant differences in cell numbers were observed between *Ol-Mlt1* mRNA-injected embryos and controls (data not shown), suggesting that the effect on cell cycle arrest observed in *Ol-insm1b* (and *Ol-insm1a*) mRNA-injected embryos is not common to all C2H2-containing proteins.

Clonal analysis of Ol-insm1b mRNA-injected embryos

Clonal analysis was performed by injecting *Ol-insm1b* mRNA in a single central blastomere at the 32-cell stage. The central blastomeres, which produce the embryo proper, are not specified at this stage (except for the germ line precursors) and proliferate actively until MBT (Thermes et al., 2006 and references therein). This experiment allowed us to follow the behaviour of *Ol-insm1b* mRNA expressing clones in a normal context. To follow the progeny of *Ol-insm1b* mRNA-injected cells, we coinjected the fluorescein-coupled control mismatch MO (MO-insm1b-C_F, 0.8 µl/ml). We used this marker instead of *EGFP* mRNA to avoid the delay due to the translation of *EGFP* into protein. Both *Ol-insm1b* mRNA-injected and control (injected with MO-insm1b-C_F alone) embryos were fixed 3 and 8 h post-injection (hpi) and counterstained with DAPI. At 3 hpi the number of cells in *Ol-insm1b*-injected clones was significantly reduced (and their size larger) when compared to control clones (in 95.6% of embryos, where 6.75±3 *versus* 37.4±8.5 cells were counted; $n=58$; Figs. 7A, C). At 8 hpi, the blastoderm covered about one half of the yolk sphere in both control and *Ol-insm1b*-injected embryos. The fluorescent cells were uniformly distributed throughout the embryo in control embryos (Fig. 7B) whereas, in *Ol-insm1b*-injected embryos, the number of fluorescent cells was strongly reduced and their distribution was not uniform throughout the blastoderm (Fig. 7D).

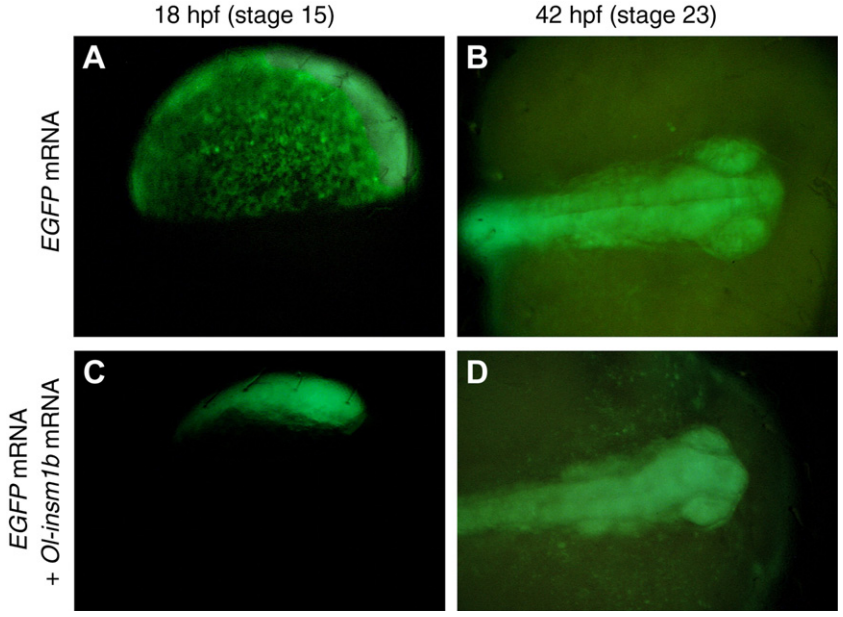

Fig. 6. Control experiments with *EGFP* mRNA. No effects on early cleavages, nor late morphological changes were observed after *EGFP* mRNA injections (A, B). Embryos coinjected with *Ol-insm1b* mRNA displayed a delayed epiboly (C) and a reduced size (D).

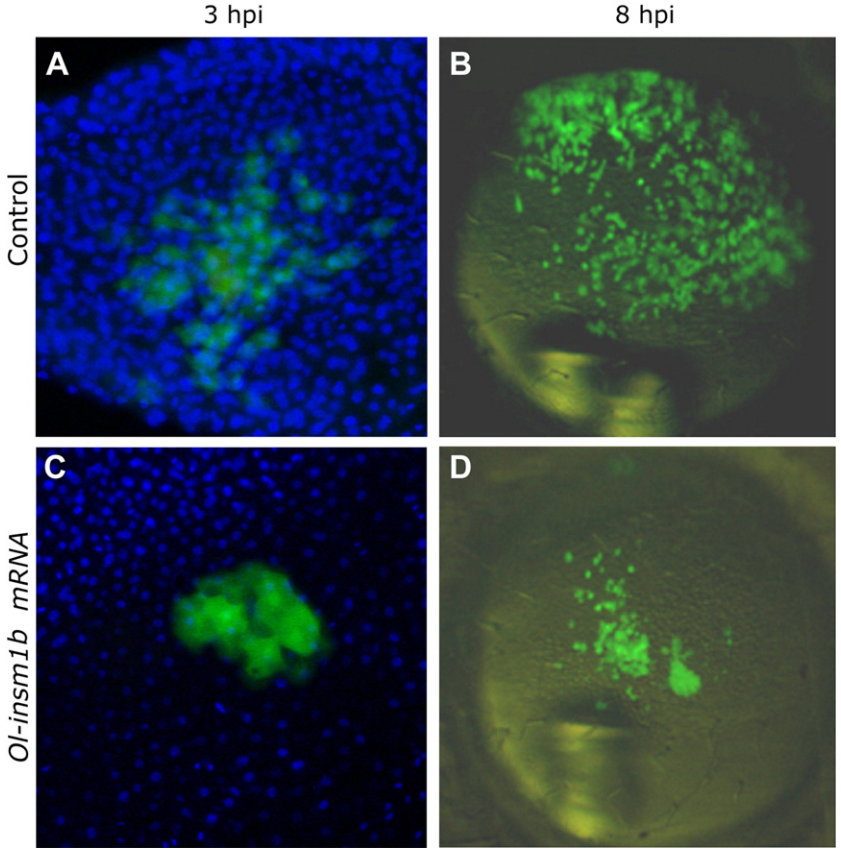

Fig. 7. Clonal analysis by injection of *Ol-insm1b* mRNA in a single central blastomere at the 32-cell stage. A clone of cells issued from a single *Ol-insm1b* mRNA-injected blastomere (500 ng/µl) contains fewer cells (C, D) than a control one (A, B). *Ol-insm1b* mRNA- and control-injected embryos were coinjected with the fluorescein-coupled control MO (MO-insm1b-C_F, green). Cells were counterstained with DAPI (blue).

Ol-insm1b mRNA injection effects on cell cycle progression

Ol-insm1b mRNA-injected (at the one-cell stage) embryos were analysed for DNA content by flow cytometry just after the mid-blastula transition (MBT; stage 11), i.e., when cell cycles become asynchronous, interphases of the cycle (G1 and G2) become detectable and apoptotic pathways become active (Fig. 8). In control embryos, nuclei were either uniformly distributed between 2N and 4N (i.e., in S phase; 55.3%) or contained 4N DNA (corresponding to cells in G2+M phase; 39.5%); a small percentage also contained 2N DNA, corresponding to cells in G1 phase (5.2%). In *Ol-insm1b* mRNA-injected embryos, we observed a decreased percentage of nuclei in S phase (25.6%) and an increased percentage of nuclei in G2+M (52.3%) and G1 (22.2%), suggesting a general shift away from proliferation.

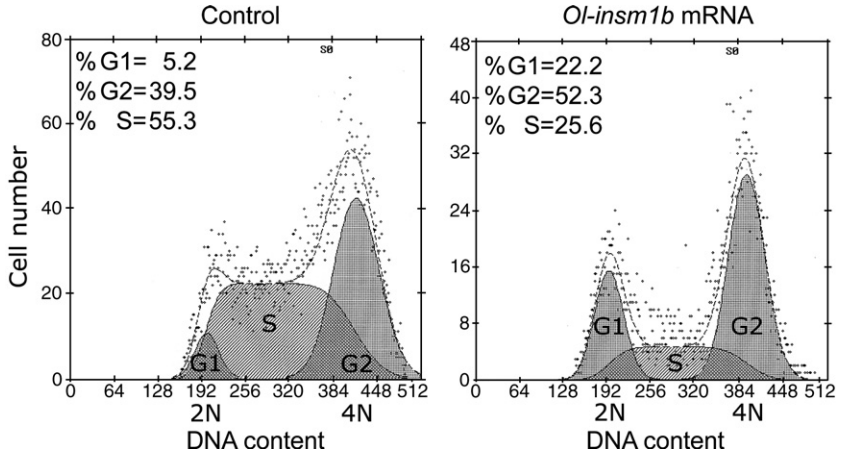

Fig. 8. Flow cytometric DNA content analysis in embryos after the MBT. DNA content histograms in a suspension of nuclei from uninjected control embryos (left) and in *Ol-insm1b* mRNA-injected embryos (right). *Ol-insm1b*-mRNA injection results in an increase in the percentage of cells in G1 and G2, and a decrease of cells in S.

Additionally, no apoptotic nuclei (i.e., no cells with DNA content inferior to 2N) were detected. These results suggest that *Ol-insm1b* affects cell proliferation since the number of cells is decreased without evidence of cell death.

Roles of the SNAG and zinc-finger domains in cell cycle arrest before MBT

To determine which of Ol-Insm1b conserved functional domains are critical for cell cycle arrest, we modified the *Ol-insm1b* sequence by deleting either the SNAG domain or the zinc-finger domains.

Embryos were injected at the one-cell stage with variable amounts of *Ol-insm1b*ΔSNAG mRNA (from 340 ng/µl to 1 µg/µl). Injection of 400 ng/µl of *Ol-insm1b*ΔSNAG caused cell cycle arrest during the first cell cleavages (in 95.2% of embryos, $n=62$; Figs. 9A, B). For comparison with *Ol-insm1b* mRNA injections, embryos were then injected with 500 ng/µl of *Ol-insm1b*ΔSNAG ($n=63$) and cells counted at 3 hpf and 5 hpf. Significant differences with cell numbers in control embryos were observed (see Table 3).

Comparable results were obtained when similar amounts of *Ol-insm1b*ΔNH_2 mRNA (lacking 207 residues in the NH2-terminus) were injected at the one-cell stage (not shown). Both *Ol-insm1b*ΔSNAG and *Ol-insm1b*ΔNH_2 constructs thus mimic the effect observed with the full-sequence *Ol-insm1b*, suggesting that the NH2-terminal domain is dispensable for the inhibition of cell division.

Table 3
Effect of deletion of conserved functional domains during pre-MBT development

	3 hpf (st. 6)	5 hpf (st. 8)
BSS	18.6±1.92	111.9±6.26
ΔSNAG mRNA 500 ng/µl, $n=63$	8.3±0.96	65.1±9.6
Δzf1–5 mRNA 500 ng/µl, $n=38$	17.2±3.13	107.7±5.91
Δzf1–2 mRNA 500 ng/µl, $n=84$	18.3±1.84	109.9±7.97

Values indicate the mean number of cells (with standard deviations) as computed in embryos injected as indicated in the left column. For each point of observation (in hours post-fertilisation; hpf), significant differences with control embryos ($P<0.0001$, Student's t test) were only detected after injection of *Ol-insm1b*ΔSNAG mRNA. *n*: total number of injected embryos.

500 ng/µl of *Ol-insm1b*Δzf1–5 mRNA was then injected at the one-cell stage (either alone or coinjected with 500 ng/µl of *EGFP* mRNA). The number of cells in *Ol-insm1b*Δzf1–5 injected embryos was not statistically different from that observed in control embryos (Table 3), suggesting that zinc-finger domains are necessary to arrest the cell cycle before MBT. Importantly, late morphological changes (after MBT) were very rarely observed and not statistically significant (Figs. 9C, D and Table 4).

We then examined whether all zinc-finger domains were necessary to arrest cell cycle. It has been shown that zinc-finger 2 of the human IA-1 protein is critical for its DNA binding activity (Breslin et al., 2003). *Ol-insm1b*Δzf1–2 mRNA was prepared by deletion of the first and second zinc-finger domains. Variable amounts of *Ol-insm1b*Δzf1–2 mRNA were injected at the one-

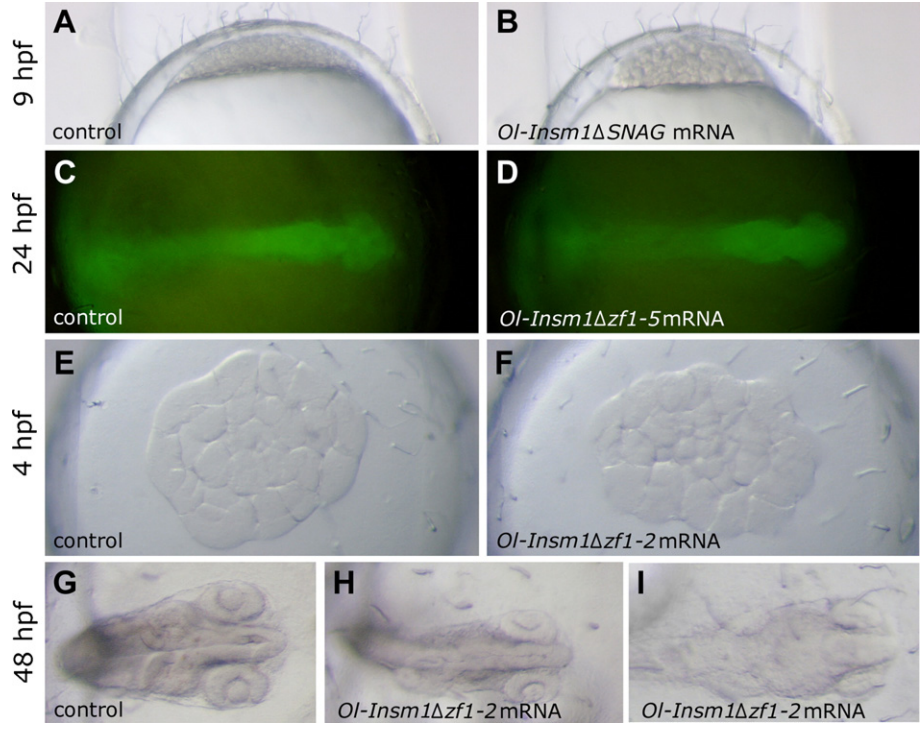

Fig. 9. Control embryos (A, C, E, G) and embryos injected with modified *Ol-insm1b* sequences lacking different functional domains (B, D, F, H, I). (B) Injection of *Ol-insm1b*Δ*SNAG* results in cell cycle arrest during the first cell cleavages. (D) Injection of *Ol-insm1b*Δ*zf1–5* mRNA does not affect development. (E, F) Significant differences between *Ol-insm1b*Δzf1–2 mRNA-injected and control embryos were never detected before MBT. (G–I) After MBT, *Ol-insm1b*Δzf1–2 mRNA-injected embryos were reduced in size (H) or showed morphological defects (I).

Table 4
Effect of deletion of conserved functional domains during post-MBT development (48 hpf)

	wt-like	Small size	Brain malformations
BSS	100%	–	–
ΔSNAG mRNA 500 ng/μl, *n*=63	–	79.4%	20.6%
Δzf1–5 mRNA 500 ng/μl, *n*=38	97.4%	2.6%	–
Δzf1–2 mRNA 375 ng/μl, *n*=39	20.5%	69.2%	10.3%
Δzf1–2 mRNA 750 ng/μl, *n*=35	–	82.4%	17.6%

Values indicate the percentage of embryos of each phenotype after injection of different constructs. A statistically significant relation was found between the injection of *Ol-insm1b*ΔSNAG mRNA and altered development after MBT ($P<0.0005$, Chi-square test). The same was found after injection of *Ol-insm1b*Δzf1–2 mRNA ($P<0.0005$, Chi-square test). In contrast, injection of *Ol-insm1b*Δzf1–5 mRNA has no statistically significance on embryonic post-MBT development. *n*: total number of injected embryos.

cell stage (from 375 ng/μl to 1 μg/μl). For comparison, 500 ng/μl injected and control embryos were allowed to develop, and cells counted at 3 and 5 hpf (see Table 3). Significant differences between *Ol-insm1b*Δzf1–2 mRNA-injected and control embryos were never detected before MBT (Table 3 and Figs. 9E, F), even when 1 μg/μl of *Ol-insm1b*Δzf1–2 of mRNA was injected (data not shown). *Ol-insm1b*Δzf1–2 mRNA-injected embryos were then allowed to develop (see Table 4) and observed at 26 hpf (st. 18; early neurula stage) and 48 hpf (stage 24; 16 somites). Embryos injected with 375 ng/μl of *Ol-insm1b* Δzf1–2 mRNA were reduced in size and/or showed morphological defects (Table 4), an effect that therefore cannot be a simple consequence of early cell cycles arrest. This effect was dose-dependant since doubling the dose of injected mRNA increased the severity of the observed phenotype (Figs. 9G–I and Table 4).

Ol-insm1b injections at the two- or four-cell stage

It has been previously reported that in zebrafish (Kimmel and Law, 1985), the early cleavages (from one-cell to 16-cell stage) are partial, with an incomplete separation of blastomeres. Accordingly, in medaka, both MO-insm1b-$_F$ and *EGFP*-mRNA spread uniformly amongst all daughter cells when injected in one blastomere of the two-cell stage or the four-cell stage embryos. To allow direct observation of *Ol-insm1b* mRNA behaviour, we prepared a pRN3-*VENUS*-*Ol-insm1b* construct in which *VENUS* was fused in frame with the *Ol-insm1b* sequence. *VENUS*-*Ol-insm1b* mRNA (500 ng/μl) was injected in one blastomere at the two-cell stage, and embryos monitored from 2 hpf to 6 hpf. Unexpectedly, VENUS-Ol-Insm1b proteins were

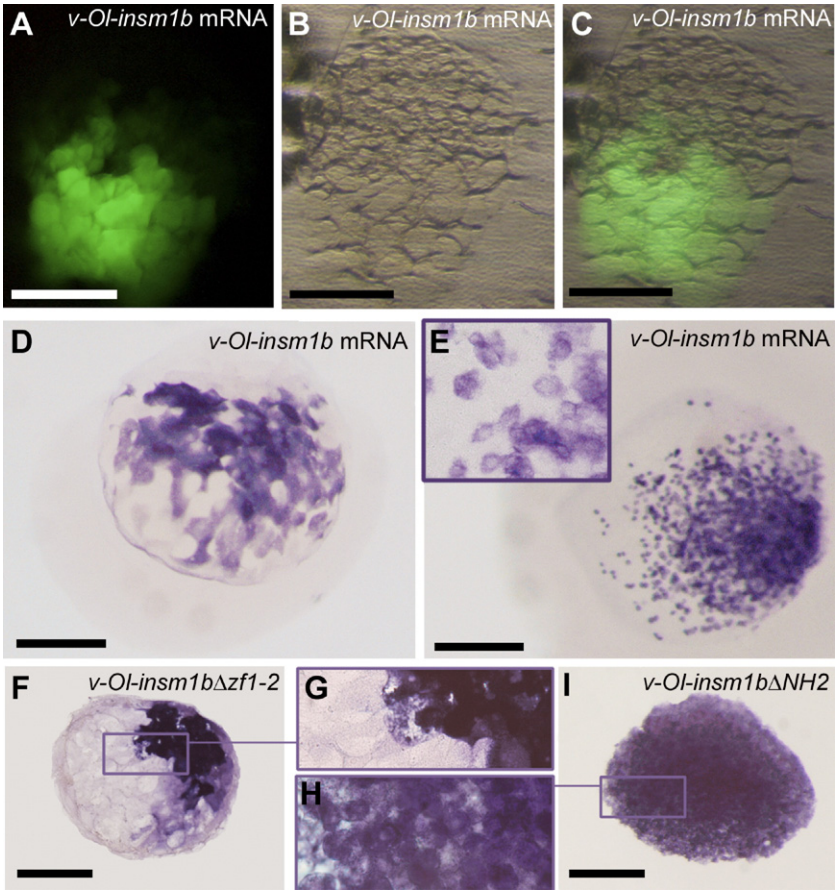

Fig. 10. (A–E) Injections of *VENUS*-*Ol-insm1b* mRNA into one blastomere at the two-cell stage. Injected mRNA does not spread in the embryo. (A–C) Fluorescence is detected in the cytoplasm of only one half of the cells, at stage 9 (5.5 hpf; 512 cells). (D, E) Dorsal views of injected embryos after WMISH performed at stage 12 (11 hpf). *Ol-insm1b* mRNA is detected in only one half of the cells. (F, G) *VENUS*-*Ol-insm1b*Δzf1–2 mRNA is also present in only one half of the cells. (H, I) *VENUS*-*Ol-insm1b*ΔNH_2 mRNA spreads uniformly amongst all cells. G and H are higher magnifications of F and I, respectively.

detected in the cytoplasm of only one half of the cells (Figs. 10A, C). We also observed that the cells derived from the injected blastomere were larger and less numerous than the cells deriving from the uninjected blastomere (Figs. 10B, C), indicating that the VENUS-Ol-Insm1b protein retained the anti-proliferative activity of Ol-Insm1b described above. Similarly, when *VENUS-Ol-Insm1b* mRNA was injected in one blastomere at the four-cell stage, fluorescence was detected in only one fourth of the cells (data not shown). Embryos injected at the two-cell stage were then fixed at 11 hpf (stage 12) and processed for WMISH using *Ol-insm1b* mRNA probes. *Ol-insm1b* mRNA expression was detected in the cytoplasm of only one half of cells (Figs. 10D, E). *VENUS-Ol-insm1b*ΔNH_2 and *VENUS-Ol-insm1b*Δzf1−2 constructs were then injected in one blastomere at the two-cell. Some embryos were then observed under fluorescence at different developmental stages and others were processed for WMISH using *Ol-insm1b* mRNA probes. While *VENUS-Ol-insm1b*Δzf1−2 mRNA was detected in only one half of cells (Figs. 10F, G), *VENUS-Ol-insm1b*ΔNH_2 appeared to spread uniformly amongst all cells (Figs. 10H, I), suggesting that the 5′ region of *Ol-insm1b* mRNA coding the SNAG domain is instrumental in preventing the spread of the mRNA to the uninjected blastomere.

Discussion

Sequence and structural features

We isolated two medaka cDNA clones (*Ol-insm1a* and *Ol-insm1b*) belonging to the *Insm1* (formerly *IA*-1) family. In all complete or nearly complete vertebrate genomes a single, intronless, *Insm1* gene is present, with the exception of the teleosts (*Tetradodon nigroviridis*, *Takifugu rubripes*, *Danio rerio* and *O. latipes*, Lukowski et al., 2006 and present study) which possess two paralogues, reflecting the well-documented genome duplication in this lineage (Wittbrodt et al., 1998).

This protein family is characterised by the presence of a SNAG (as present in all **Sna**il/Slu**g** vertebrate proteins; Grimes et al., 1996) motif at the amino-terminal end and five zinc-fingers of the Cys2-His2 type at the carboxy-terminal end. Their SNAG domain (MPKGFLV) is typical of the Mlt1/Insm1 subfamily: in Snail/Slug/Scratch proteins and Gfi1 proteins, the SNAG domain is MPRSFLV. This domain is essential for the repressor activity of Gfi1 proteins, independently from the identity of its fourth amino acid (Grimes et al., 1996). Additionally, a conservative substitution is present in Ol-Insm1b SNAG (MPKGFLV), as in the zebrafish Dr-Insm1b. A putative nuclear localisation signal (NLS) upstream of zinc-finger 1 is present in Ol-Insm1b and Ol-Insm1a, as in all other members of the Mlt1/Insm1 group, but not in Snail/slug/Scratch or Gfi proteins. The other recognisable motifs in Ol-Insm1b and Ol-Insm1a are the zinc-fingers (Miller et al., 1985; Goto et al., 1992). In Ol-insm1a and Ol-insm1b, as in their mammalian counterparts, a conserved arginine residue replaces the second histidine of zinc-finger 1. In addition, the third zinc-finger is spaced roughly at equal distance from the two tandem repeated zinc-finger motifs located at each side, a feature that may suggest a precise mode of DNA binding. A peculiarity of Ol-Insm1b is the presence of a serine-rich sequence (SSSSSSSLA-SSSSSSSSSSSS) upstream of zinc-finger 4; such a stretch of amino acids is not present in either Ol-Insm1a, zebrafish or mammalian Insm1 proteins.

The nomenclature of this molecule family is not fully standardised; indeed, in a recent paper (Lukowski et al., 2006) its zebrafish members (Dr-Insm1a and Dr-Inms1b) are considered to belong to the EIN (rather than the SNAG) protein family, based on the sequence similarity of the zinc-fingers with those of the EGF-46 (from *Caenorhabditis*) and Nerfin-1 (from *Drosophila*) proteins. We decided to stick with the SNAG nomenclature (Grimes et al., 1996), mostly because of the results of our functional analyses.

Finally, we chose to match the names (1a and 1b) of the two medaka paralogues with those of their zebrafish counterparts based on: (i) sequence data, notably the above-mentioned substitution in the SNAG domain, and (ii) expression data; indeed, we have found that *Ol-insm1b* is not expressed until the end of gastrulation. This is in contrast with zebrafish *Dr-insm1a*, whose transcripts appear to be maternally contributed, whilst those of *Dr-insm1b* are not (Lukowski et al., 2006).

Expression domains and time course

We have performed a detailed analysis of *Ol-insm1b* expression by WMISH in embryos and on histological sections of adult brains. From this point of view also, *Ol-insm1b* is a typical member of the *Insm1* gene family: besides a strong and conserved expression in the developing pancreas, its transcripts are especially prominent in the CNS during the neurogenetic period (Candal et al., 2005a). *Ol-insm1b* expression is especially strong in the OT arrest zone as soon as this later becomes detectable (Nguyên et al., 2001a), and in the developing hindbrain, where it exhibits a transient banded pattern previously found in other negative cell cycle regulators such as *Ol-KIP* and *Ol-Gadd45*γ (Nguyên et al., 2001b; Candal et al., 2004, 2005a). *Ol-insm1b* expression peaks at late somitogenesis stages and then decreases as differentiation proceeds; it is turned off in most terminally differentiated cells. *Ol-insm1b* continues to be strongly expressed in the medaka adult CNS, in a pattern similar to that observed in embryos, albeit with some differences: notably, *Ol-insm1b* mRNA is strongly and asymmetrically expressed in the left habenula of the adult brain, whereas its expression is symmetrical in the development of this diencephalic structure. Structural asymmetries (notably in size) in the habenula are widespread amongst vertebrates (Concha and Wilson, 2001). While in medaka embryos the anlagen of the right and left habenulas are similar in size, in adult brains, the left habenula is clearly smaller than the right one (see Fig. 3), as it is in other teleosts (*Salmo trutta fario*; Candal, 2002). This late appearance of a size asymmetry is concomitant with the late asymmetry in *Ol-insm1b* expression. Given its role in cell proliferation control (see below), it is tempting to propose that *Ol-insm1b* precocious expression in the smaller (left) habenula is linked with an earlier arrest of cell cycle leading to its final smaller size, an intriguing hypothesis which remains to be tested.

Overall, *Ol-insm1b* expression pattern closely resembles that of zebrafish *Dr-insm1a* and *Dr-insm1b* (Lukowski et al., 2006), both spatially (expression domains, prominence in the pancreas and CNS) and temporally (overall time course, peak at neurogenesis and later decrease).

These features are found beyond the teleostean lineage: in mouse, *Insm1* transcripts are detected from embryonic day 10.5 until 2 weeks post-partum, notably in the brain (Xie et al., 2002; Breslin et al., 2003). Mammalian *Insm1* is also expressed in foetal pancreas, foetal brain and tumors of neuroendocrine origin (for example mouse pituitary tumor, rat medullary thyroid carcinoma and human small cell lung carcinoma), but not in most non-neuroendocrine tumors or normal adult tissues (including pancreas and brain; Goto et al., 1992; Lan et al., 1993, 1994).

These expression studies thus clearly point to a likely role for the *insm1* genes in CNS neurogenesis. In contrast with the mammalian situation, we also detected a strong expression of *Ol-insm1b* in the adult brain. It is quite possible that, since neurogenesis is continuous in teleosts (Wullimann and Puelles, 1999; Zupanc, 1999; Wullimann and Knipp, 2000; Ekström et al., 2001; Nguyên et al., 2001a; Candal et al., 2005c) this expression simply reflects a different mode of brain growth between teleosts and mammals.

Functional analysis

In vitro studies showed that Insm1 is a transcriptional repressor (as are most if not all members of the SNAG family) and that it regulates the *NeuroD1* gene, an important factor in pancreatic and neural development (Breslin et al., 2002, 2003); it is also a target of *Neurogenin3* and is required for normal differentiation of pancreatic endocrine cells *in vitro* (Mellitzer et al., 2006). However, to our knowledge, the role of Insm1 proteins *in vivo* has never been analysed.

Our first choice was to over-express *Ol-insm1b* in a cellular context as close as possible as its physiological one, i.e., in neural progenitors. To this aim, we generated transgenic F0 embryos where the expression of a *VENUS-Ol-insm1b* fusion transgene was driven specifically in CNS proliferating cells by the α1-tubulin promoter (Gloster et al., 1994, 1999). The clear correlation between the fluorescence intensity in these embryos and the reduction in size of their nervous system further points to a role of *Ol-insm1b* in negative cell cycle control. However, it was difficult to analyse these effects at a cellular level in these mosaic embryos. We could not produce a stable transgenic line with the α1-tubulin-*VENUS-Ol-insm1b* construct, the ubiquity (as far as the CNS is concerned) and strength of the promoter (as seen in our mosaic F0 embryos) affecting the viability of such transgenic animals. We thus turned to experiments involving over-expression in pre-MBT embryos, by mRNA injection at the one-cell stage, a technique commonly used in fish and amphibian models. Admittedly, these experiments are less "physiological" because *Ol-insm1b* expression starts at neurula stages. They still represent ectopic expressions in an *in vivo* context and allowed us to undertake a dissection of Ol-Insm1b functional domains. A strong generalised ectopic expression (injection at the one-cell stage) slows down early development in a dose-dependent manner. This effect is strictly cell-autonomous, as demonstrated by clonal experiments (injection of *Ol-insm1b* mRNA in a single cell at the 32-cell stage). Flow cytometry showed that *Ol-insm1b* causes a general shift away from proliferation. Importantly, we never observed any evidence of apoptosis in these experiments.

These results suggest that *Ol-insm1b* negatively regulates cell proliferation in early embryos. It is of special importance to emphasise that, whilst zinc-finger-containing proteins are best known as transcriptional regulators, these strong effects of *Ol-insm1b* on cell cycle were observed despite Insm1 proteins were localised only in the cytoplasm. We were therefore confronted to the seemingly paradoxical result of a likely transcriptional repressor having a strong anti-proliferative effect in a largely transcription-free context. This prompted us to check which domains of Ol-Insm1b were responsible for its action.

The SNAG domain of various Snag and Gfi1 proteins is essential for their repressor activity (Grimes et al., 1996; Nakayama et al., 1998; Okubo et al., 2001; Tateno et al., 2001; Peinado et al., 2004; Fiolka et al., 2006). However, Snail and Gfi1 proteins depend on the presence of the SNAG *and* the zinc-finger domains for maximum repressor effect (Nakayama et al., 1998; Tateno et al., 2001; McGee et al., 2003). We deleted these domains of Ol-Insm1b to assess their functions *in vivo*.

The effects of constructs devoid of the SNAG domain are identical, on pre-MBT embryos, to those of the full sequence. Therefore, Ol-Insm1b negative effect on cell cycle progression is not mediated by the SNAG domain.

Conversely, embryos injected with a construct lacking the five zinc-fingers develop normally both before and after MBT, suggesting that the zinc-finger motifs (or some of them) are necessary for the autonomous, transcription-independent cell cycle arrest in pre-MBT embryos.

It has been shown that zinc-finger 2 of the human IA-1/Insm1 protein is critical for its activity (Breslin et al., 2003); we thus checked the effects of *Ol-insm1b*Δzf1–2: embryos injected with this construct develop normally before (but not after) MBT, indicating that that zinc-finger 2 is necessary for cell cycle arrest before MBT.

Furthermore, this strong anti-proliferative effect appears to be specific of the Ol-Insm1b protein. Indeed, it is not mimicked by injecting *Ol-Mlt1* mRNA in the same conditions: this gene, which is molecularly the "closest relative" of *Ol-insm1* within the SNAG family, does not induce any developmental delay.

These results show that Ol-Insm1b acts in pre-MBT embryos via its zinc-finger motifs in a transcription-independent way. This is also in good agreement with the cytoplasmic localisation of the fusion protein observed in injections performed in one-cell at the two-cell stages. A possible clue to this apparently paradoxical phenomenon lies in the fact that C2H2-type zinc-fingers are amongst the very few (the only others are the U1-like type) to specifically bind both DNA and RNA, whilst 44 additional families of zinc-finger proteins have been implicated in either DNA–protein, protein–protein or protein–lipid binding (Ravasi et al., 2003). For example, TFIIIA (the archetype of the C2H2-containing proteins; Miller et al., 1985) is a dual RNA/

DNA-binding protein where individual C2H2 fingers make different contacts with one or another nucleic acid, i.e., fingers 1–3 bind strongly to DNA, and central fingers 4–6 bind to RNA (Searles et al., 2000; Brown, 2005). Although further studies are clearly needed to elucidate the underlying mechanism(s), a working hypothesis might therefore be that Ol-Insm1b negatively regulates cell proliferation through a protein–RNA interaction rather than, or in addition to, a DNA-binding-based mechanism.

When observed after gastrulation, embryos injected with the full-length *Ol-insm1b* mRNA showed a dramatically reduced size. While this may be due to the early (pre-MBT) decrease in cell numbers, it also suggested late, or maintained, effects since embryos have normally amazing capacities of recovery. This hypothesis was strengthened by the injections of *Ol-insm1b* Δzf1–2 constructs: in this case, embryos developed normally *before* MBT, but exhibited a reduction in size and/or morphological defects *after* MBT. In this case, their reduced size could therefore not be due to early cell cycles arrest. This can be taken as an additional indication for an anti-proliferative role of *Ol-insm1b*, a hypothesis that indeed appears compatible with all experiments reported here.

An unexpected restriction of diffusion in early development

In medaka, as in zebrafish (Kimmel and Law, 1985), the early cleavages (1-cell to 16-cell stage) are partial, and molecules such as mRNA or morpholinos spread uniformly amongst all daughter cells when injected in one blastomere of the 2- to 16-cell stage embryos (Candal et al., 2004 and present results). Surprisingly, when we injected a pRN3-*VENUS*-*Ol-insm1b* fusion construct in one out of two, or one out of four blastomeres, we subsequently observed fluorescence in the cytoplasm of only one half or one fourth of the daughter cells, respectively; these cells were also larger and less numerous, as expected given our previous observations. The same restriction was observed, by ISH, for the *VENUS*-*Ol-insm1b* mRNA, suggesting that the mRNAs, rather than the proteins, are diffusion-restricted. We then checked the effects of deleted constructs: whereas *VENUS*-*Ol-insm1b*Δzf1–2 (lacking the first and second zinc-fingers) behaves identically to the full construct, *VENUS*-*Ol-insm1b*ΔNH_2 (lacking the NH2 terminal, including the SNAG domain) leads to a uniform diffusion, both at the mRNA and protein levels. This suggests that the signal(s) for restricting the diffusion in early blastomeres are located at the 5′ end of the *Insm1* mRNA molecule. *Subcellular* localisation of mRNAs is a well-documented phenomenon, and it has been shown to be largely dependent on signals located in the 3′ UTR of these molecules (Kloc et al., 2002; Van de Bor and Davis, 2004); however, here the uneven mRNA distribution is observed between different cells rather than between different compartments of the same cell. More experiments are needed to elucidate this phenomenon, which, to our best knowledge, has not been reported before.

Our results thus indicate that *Ol-insm1b* is likely to play a role in vertebrate development as a novel anti-proliferative molecule: it functions as a negative regulator of the cell cycle, without triggering the apoptotic pathway. At least part of this effect is mediated by Ol-Insm1b zinc-finger domains, but not via a transcriptional mechanism. These results, added to the already documented correlation between the deregulation of *Insm1* and neuroendocrine tumour progression in vertebrates, open new perspectives in the field of cancer studies.

Acknowledgments

We wish to thank Carole Deyts for major contribution to WMISH, Laurent Legendre for skilful maintenance of fish and Philippe Vernier for support. We are grateful to Spencer Brown and Olivier Catrice for assistance in flow cytometry analyses. This work was supported by the European Commission (EaC key action QLK3-CT-2001-01890 and Plurigenes STREP project LSHG-CT-2005-018673), INRA, CNRS, INSERM and University Paris-Sud.

References

Ashraf, S.I., Ganguly, A., Roote, J., Ip, Y.T., 2004. Worniu, a Snail family zinc-finger protein, is required for brain development in *Drosophila*. Dev. Dyn. 231, 379–386.

Breslin, M.B., Zhu, M., Notkins, A.L., Lan, M.S., 2002. Neuroendocrine differentiation factor, IA-1, is a transcriptional repressor and contains a specific DNA-binding domain: identification of consensus IA-1 binding sequence. Nucleic Acid Res. 30, 1038–1045.

Breslin, M.B., Zhu, M., Lan, M., 2003. NeuroD/E47 regulates the E-box element of a novel zinc finger transcription factor IA-1, in developing nervous system. J. Biol. Chem. 278, 38991–38997.

Brown, R., 2005. Zinc finger proteins: getting a grip on RNA. Curr. Opin. Struct. Biol. 15, 94–98.

Calle-Mustienes, E., Glavic, A., Modolell, J., Gómez-Skarmeta, J.L., 2002. Xiro homoproteins coordinate cell cycle exit and primary neuron formation by upregulating neuronal-fate repressors and downregulating the cell-cycle inhibitor XGadd45-γ. Mech. Dev. 119, 69–80.

Candal, E., 2002. Proliferation and cell death in the brain and retina of teleosts: relation to *Ol-KIP* and *reelin* expression. Ph. D. Thesis, Santiago de Compostela.

Candal, E., Thermes, V., Joly, J.S., Bourrat, F., 2004. Medaka as a model for the characterization of cell cycle regulators: a functional analysis of Ol-Gadd45γ during embryogenesis. Mech. Dev. 121, 945–958.

Candal, E., Nguyên, V., Joly, J.S., Bourrat, F., 2005a. Expression domains suggest cell-cycle independent roles of growth-arrest molecules in the adult brain of the medaka, *Oryzias latipes*. Brain Res. Bull. 66, 426–430.

Candal, E., Anadón, R., De Grip, W.J., Rodríguez-Moldes, I., 2005b. Patterns of cell proliferation and cell death in the developing retina and optic tectum of the brown trout. Dev. Brain Res. 154, 101–119.

Candal, E., Anadon, R., Bourrat, F., Rodriguez-Moldes, I., 2005c. Cell proliferation in the developing and adult hindbrain and midbrain of trout and medaka (teleosts): a segmental approach. Brain Res. Dev. Brain Res. 160, 157–175.

Carey, R.G., Li, B., DiCicco-Bloom, E., 2002. Pituitary adenylate cyclase activating polypeptide anti-mitogenic signaling in cerebral cortical progenitors is regulated by p57Kip2-dependent CDK2 activity. J. Neurosci. 22, 1583–1591.

Carter, A.D., Sible, J.C., 2003. Loss of XChk function triggers apoptosis after the midblastula transition in *Xenopus laevis* embryos. Mech. Dev. 120, 315–323.

Caviness Jr., V.S., Takahashi, T., Nowakowski, R.S., 2000. Neurogenesis and the early events of neocortical histogenesis. Results Probl. Cell Differ. 30, 107–143.

Concha, M.L., Wilson, S.W., 2001. Asymmetry in the epithalamus of vertebrates. J. Anat. 199, 63–84.

Deyts, C., Candal, E., Joly, J.S., Bourrat, F., 2005. An automated *in situ*

hybridization screen in the medaka to identify unknown neural genes. Dev. Dyn. 234, 698–708.
Dyer, M.A., Cepko, C.L., 2000. p57 (kip2) regulates progenitor cell proliferation and amacrine interneuron development if the mouse retina. Development 127, 3593–3605.
Ekström, P., Johnsson, C.M., Ohlin, L.M., 2001. Ventricular proliferation zones in the brain of an adult teleost fish and their relation to neuromeres and migration (secondary matrix zones). J. Comp. Neurol. 436, 92–110.
Fiolka, K., Hertzano, R., Vassen, L., Zeng, H., Hermesh, O., Abraham, K.B., Duhrsen, U., Moroy, T., 2006. Gfi1 and Gfi1b act equivalently in haematopoiesis, but have distinct, non-overlapping functions in inner ear development. EMBO Rep. 7, 326–333.
Galbraith, D.W., Harkins, K.R., Maddox, J.R., Ayres, N.M., Sharma, D.P., Firoozabady, E., 1983. Rapid flow cytometric analysis of the cell cycle in intact plant tissues. Science 220, 1049–1051.
Gloster, A., Wu, W., Speelnan, A., Weiss, S., Causing, C., Pozniak, C., Reynolds, B., Chang, E., Toma, J.C., Miller, F.D., 1994. The T1α α-tubulin promoter specifies gene expression as a function of neuronal growth and regeneration in transgenic mice. J. Neurosci. 14, 7319–7330.
Gloster, A., El-Bizri, H., Barnji, S.X., Rogers, D., Miller, F.D., 1999. Early induction of Tα1 α-tubulin transcription in neurons of the developing nervous system. J. Comp. Neurol. 405, 45–60.
Goto, Y., De Silva, M.G., Toscani, A., Prabhacar, B.S., Notkins, A.L., Lan, M.S., 1992. A novel human insulinoma-associated cDNA, IA-1, encodes a protein with "zinc-finger" DNA-binding motifs. J. Biol. Chem. 267, 15252–15257.
Grabher, C., Joly, J.S., Wittbrodt, J., 2004. Highly efficient zebrafish transgenesis mediated by the meganuclease I-SceI. Methods Cell Biol. 77, 381–401.
Grimes, H.L., Chan, T.O., Zweiler-McKay, P.A., Tong, B., Tsichlis, P.N., 1996. The Gfi-1 proto-oncoprotein contains a novel transcriptional repressor domain, SNAG, and inhibits G1 arrest induced by interleukin-2 withdrawal. Mol. Cell Biol. 16, 6263–6272.
Hardcastle, Z., Papalopulu, N., 2000. Distinct effects of *XBF-1* in regulating the cell cycle inhibitor $p27^{Xic1}$ and imparting a neural fate. Development 127, 1303–1314.
Hensey, C., Gautier, J., 1997. A developmental timer that regulates apoptosis at the onset of gastrulation. Mech. Dev. 69, 183–195.
Hieber, V., Dai, X., Foreman, M., Goldman, D., 1998. Induction of alpha1-tubulin gene expression during development and regeneration of the fish nervous system. J. Neurobiol. 137, 429–440.
Hock, H., Hamblen, M.J., Rooke, H.M., Schindler, J.W., Saleque, S., Fujiwara, Y., Orkin, S.H., 2004. Gfi-1 restricts proliferation and preserves functional integrity of haematopoietic stem cells. Nature 431, 1002–1007.
Huynh, H.T., Teel, R.W., 2000. Selective induction of apoptosis in human mammary cancer cells (MCF-7) by pycnogenol. Anticancer Res. 20, 2417–2420.
Iwamatsu, T., 1994. Stages of normal development in the medaka *Oryzias latipes*. Zool. Sci. 11, 825–839.
Joly, J.S., Bourrat, F., Nguyen, V., Chourrout, D., 1997. Ol-Prx3, a member of an additional class of homeobox genes, is unimodally expressed in several domains of the developing and adult central nervous system of the medaka (*Oryzias latipes*). Proc. Natl. Acad. Sci. U. S. A. 94, 12987–12992.
Kango-Sinh, M., Nolo, R., Tao, C., Verstreken, P., Hiesinger, P.R., Bellen, H.J., Halder, G., 2002. Shar-pei mediates cell proliferation arrest during imaginal disc growth in *Drosophila*. Development 129, 5719–5730.
Kimmel, C.B., Law, R.D., 1985. Cell lineage of zebrafish blastomeres: I. Cleavage pattern and cytoplasmatic bridges between cells. Dev. Biol. 108, 78–85.
Kloc, M., Zearfoss, N.R., Etkin, L.D., 2002. Mechanisms of subcellular mRNA localization. Cell 108, 533–544.
Lan, M.S., Russell, E.K., Ku, J., Johnson, B.E., Notkins, A.L., 1993. IA-1, a new marker for neuroendocrine differentiation in human lung cancer cell lines. Cancer Res. 53, 4169–4171.
Lan, M.S., Li, Q., Lu, J., Modi, W.S., Notkins, A.L., 1994. Genomic organization, 59-upstream sequence, and chromosomal location of an insulinoma-associated intronless gene, *IA-1*. J. Biol. Chem. 269, 14170–14174.
Lemaire, P., Garrett, N., Gurdon, J.B., 1995. Expression cloning of Siamois, a *Xenopus* 2 Homeobox gene expressed in dorsal–vegetal cells of blastulae and able to induce a complete secondary axis. Cell 81, 85–94.
Li, Q., Notkins, A.L., Lan, M.S., 1997. Molecular characterization of the promoter region of a neuroendocrine tumor marker, IA-1. Biochem. Biophys. Res. Commmun. 236, 776–781.
Lukowski, C.M., Ritzel, R.G., Waskiewick, A.J., 2006. Expression of two *insm1*-like genes in the developing zebrafish nervous system. Gene Exp. Patterns 6, 711–718.
McGee, L., Bryan, J., Elliot, L., Grimes, H.L., Kazanjian, A., Davis, J.N., Meyers, S., 2003. Gfi-1 attaches to the nuclear matrix, associates with ETO (MTG8) and histone deacetylase proteins, and repress transcription using a TSA-sensitive mechanism. J. Cell Biochem. 89, 1005–1018.
Mellitzer, G., Bonne, S., Luco, R.F., Van De Casteele, M., Lenne-Samuel, N., Collombat, P., Mansouri, A., Lee, J., Lan, M., Pipeleers, D., Nielsen, F.C., Ferrer, J., Gradwohl, G., Heimberg, H., 2006. IA1 is NGN3-dependent and essential for differentiation of the endocrine pancreas. EMBO J. 25, 1344–1352.
Miller, J., McLachlan, A.D., Klug, A., 1985. Repetitive zinc-binding domains in the proteins transcription factor IIIA from *Xenopus* oocytes. EMBO J. 4, 1609–1614.
Nagai, T., Ibata, K., Park, E.S., Kubota, M., Moshiba, K., Miyawaki, A., 2002. A variant of yellow fluorescent protein with fast and efficient mutation for cell biological applications. Nat. Biotechnol. 20, 87–90.
Nakakura, E.K., Watkins, D.N., Schuebel, K.E., Sriuranpong, V., Borges, M.W., Nelkin, B.D., Ball, D.W., 2001a. Mammalian scratch: a neural-specific Snail family transcriptional repressor. Proc. Natl. Acad. Sci. U. S. A. 98, 4010–4015.
Nakakura, E.K., Watkins, D.N., Sriuranpong, V., Borges, M.W., Nelkin, B.D., Ball, D.W., 2001b. Mammalian scratch participates in neuronal differentiation in P19 embryonal carcinoma cells. Brain Res. Mol. Brain Res. 95, 162–166.
Nakayama, H., Scott, I.C., Cross, J.C., 1998. The transition to endoreplication in trophoblast giant cells is regulated by the mSNA zinc finger transcription factor. Dev. Biol. 199, 150–163.
Nguyên, V., Deschet, K., Henrich, T., Godet, E., Joly, J.S., Wittbrodt, J., Chourrout, D., Bourrat, F., 1999. Morphogenesis of the optic tectum of the medaka (*Oryzias latipes*): a morphological and molecular study, with special emphasis on cell proliferation. J. Comp. Neurol. 413, 385–404.
Nguyên, V., Joly, J.S., Bourrat, F., 2001a. An *in situ* screen for genes controlling cell proliferation in the optic tectum of the medaka (*Oryzias latipes*). Mech. Dev. 107, 55–67.
Nguyên, V., Candal-Suárez, E.M., Sharif, A., Joly, J.S., Bourrat, F., 2001b. Expression of Ol-KIP, a cyclin-dependent kinase inhibitor, in embryonic and adult medaka (*Oryzias latipes*) central nervous system. Dev. Dyn. 222, 439–449.
Ogino, H., McConnell, W.B., Grainger, R.M., 2006. Highly efficient transgenesis in *Xenopus tropicalis* using I-*Sce*I meganuclease. Mech. Dev. 123, 103–113.
Okubo, T., Truong, T.K., Yu, B., Itoh, T., Zhao, J., Grube, B., Zhou, D., Chen, S., 2001. Down-regulation of promoter 1.3 activity of the human aromatase gene in breast tissue by zinc-finger protein, snail (SnaH). Cancer Res. 61, 1338–1346.
Pan, F.C., Chen, Y., Loeber, J., Henningfeld, K., Pieler, T., 2006. I-SceI meganuclease-mediated transgenesis in *Xenopus*. Dev. Dyn. 235, 247–252.
Park, J.H., Sung, I.J., Lee, S.W., Kim, K.W., Kim, Y.S., Yoo, M.A., 2005. The zinc-finger transcription factor Snail downregulates proliferating cell nuclear antigen expression in colorectal carcinoma cells. Int. J. Oncol. 26, 1541–1547.
Peinado, H., Ballestar, E., Esteller, M., Cano, A., 2004. Snail mediates E-cadherin repression by recruitment of the SinA3/histone deacetylase 1 (HDAC1)/HDAC2 complex. Mol. Cell Biol. 24, 306–319.
Ravasi, T., Huber, T., Zavolan, M., Forrest, A., Gaasterland, T., Grimmond, S., RIKEN GER Group, GSL Members, Hume, D., 2003. Systematic characterization of the zinc-finger-containing proteins in the mouse transcriptome. Genome Res. 13, 1430–1442.
Retief, J.D., 2000. Phylogenetic analysis using PHYLIP. Methods Mol. Biol. 132, 243–258.
Searles, M.A., Lu, D., Klug, A., 2000. The role of the central zinc fingers of transcription factor IIIA in binding 5S RNA. J. Mol. Biol. 301, 47–60.
Sefton, M., Sanchez, S., Nieto, M.A., 1998. Conserved and divergent roles for

members of the snail family of transcription factors in the chick and mouse embryo. Development 125, 3111–3121.

Stegmann, K., Boecker, J., Kosman, C., Ermert, A., Kunz, J., Koch, M.C., 1999. Human transcription factor SLUG: mutation analysis in patients with neural tube defects and identification of a missense mutation (D119E) in the Slug subfamily-defining region. Mutat. Res. 406, 63–69.

Takahashi, E., Funato, N., Higashihori, N., Hata, Y., Gridley, T., Nakamura, M., 2004. Snail regulates p21 (WAF/CIP1) expression in cooperation with E2A and Twist. Biochem. Biophys. Res. Commun. 325, 1136–1144.

Tateno, M., Fukunishi, Y., Komatsu, S., Okazaki, Y., Kawai, J., Shibata, K., Itoh, M., Muramatsu, M., Held, W.A., Hayashizaki, Y., 2001. Identification of a novel member of the Snail/Gfi repressor family, *mlt 1*, which is methylated and silenced in liver tumors of SV40 T antigen transgenic mice. Cancer Res. 61, 1144–1153.

Thermes, V., Grabher, C., Ristoratore, F., Bourrat, F., Choulika, A., Wittbrodt, J., Joly, J.S., 2002. I-SceI meganuclease mediates highly efficient transgenesis in fish. Mech. Dev. 118, 91–98.

Thermes, V., Candal, E., Alunni, A., Serin, G., Bourrat, F., Joly, J.S., 2006. Medaka simplet (FAM53B) belongs to a family of novel vertebrate genes controlling cell proliferation. Development 133, 1881–1890.

Thompson, J.D., Higgins, D.G., Gibson, T.J., 1994. CLUSTAL W: improving the sensitivity of progressive multiple sequence alignment through sequence weighting, position-specific gap penalties and weight matrix choice. Nucleic Acids Res. 22, 4673–4680.

Tong, B., Grimes, H.L., Yang, T., Bear, S., Qin, Z., Du, K., El-Deiry, W.S., Tsichlis, P.N., 1998. The Gfi-1B proto-oncoprotein represses p21WAF1 and inhibition. Mol. Cell. Biol. 18, 2462–2473.

Van de Bor, V., Davis, I., 2004. mRNA localization gets more complex. Curr. Opin. Cell Biol. 16, 300–307.

Wittbrodt, J., Meyer, A., Schartl, M., 1998. More genes in fish? Bioessays 20, 511–515.

Wittbrodt, J., Shima, A., Schartl, M., 2002. Medaka, a model organism from the Far East. Nat. Rev. Genet. 1, 53–64.

Wu, W.S., Heinrichs, S., Xu, D., Garrison, S.P., Zambetti, G.P., Adams, J.M., Look, A.T., 2005. Slug antagonizes p53-mediated apoptosis of hematopoietic progenitors by repressing puma. Cell 123, 641–653.

Wullimann, M.F., Knipp, S., 2000. Proliferation pattern changes in the zebrafish brain from embryonic through early postembryonic stages. Anat. Embryol. 202, 385–400.

Wullimann, M.F., Puelles, L., 1999. Postembryonic neural proliferation in the zebrafish forebrain and its relation to prosomeric domains. Anat. Embryol. 329, 329–348.

Xie, J., Cai, T., Zhang, H., Lan, M.S., Notkins, A.L., 2002. The zinc-finger transcription factor INSM1 is expressed during embryo development and interacts with the Cbl-associated protein. Genomics 80, 54–61.

Yamamoto, T., 1975. Medaka (killifish) Biology and Strains. Keigaku, Tokyo.

Zong, W.X., Li, C., Hatzivassiliou, G., Lindsten, T., Yu, Q.C., Yuan, J., Thompson, C.B., 2003. Bax and Bak can localize to the endoplasmic reticulum to initiate apoptosis. J. Cell Biol. 162, 59.

Zupanc, G.H.K., 1999. Neurogenesis, cell death and regeneration in the adult gymnotiform brain. J. Exp. Biol. 202, 1435–1446.